Fate of calcareous nannofossils during the Rhaetian (Late Triassic): evidence from the Northern Calcareous Alps, Austria

Isaline Demangel, Zsófia Kovács, Silvia Gardin, Leopold Krystyn, Werner E Piller, Andre Baldermann, Sylvain Richoz

Lethaia
AN INTERNATIONAL JOURNAL OF PALAEONTOLOGY AND STRATIGRAPHY

Fate of calcareous nannofossils during the Rhaetian (Late Triassic): evidence from the Northern Calcareous Alps, Austria

ISALINE DEMANGEL, ZSÓFIA KOVÁCS, SILVIA GARDIN, LEOPOLD KRYSTYN, WERNER E. PILLER, ANDRE BALDERMANN, SYLVAIN RICHOZ

LETHAIA

Calcareous nannofossils evolved in the global ocean from the Carnian (early Late Triassic) and have contributed to the accumulation of biogenic calcium carbonate in marine sediments since then. Bio-diversification and bio-productivity became more significant in the Rhaetian (Late Triassic), representing an important period to understand the dynamics of calcareous nannofossil evolution. The calcareous nannofossil content of the Zlambach Formation, Northern Calcareous Alps, Austria, was qualitatively and quantitatively investigated using both scanning electron and light microscopy. The nannolith, *Prinsiosphaera triassica triassica,* dominates the assemblage in most samples and increases slightly in abundance in the lower Rhaetian, followed by a small-scale short-term increase during the middle Rhaetian and reaches rock-forming abundance in the upper Rhaetian. A systematic size decrease is recorded from the lower Rhaetian onwards, possibly due to changes in the palaeo-environment. The abundance of *P. triassica triassica* is slightly affected by the occurrence of *Eoconusphaera hallstattensis* and strongly by *E. zlambachensis*. *E. hallstattensis* is constrained to a relatively short interval, from the upper *Paracochloceras suessi* Zone (lower Rhaetian) and disappeared during the lower *Vandaites stuerzenbaumi* Zone (middle Rhaetian), after the occurrence of a second Eoconusphaeraceae species*: E. zlambachensis.* The last occurrence of *E. hallstattensis* comes along with the subspecies *Prinsiosphaera triassica crenulata* showing characteristic parallel-oriented calcite lamellae. Those three species are suggested as good biostratigraphical markers for the Upper Triassic. The coccolithophorids are present in low abundance, increasing slightly in the middle Rhaetian. After the first record of coccoliths in the middle Norian (Alaunian), the oldest *Crucirhabdus minutus* and *Archaeozygodiscus koessenensis* were observed in the upper Norian (Sevatian) and the first occurrence of *Crucirhabdus primulus* was recorded in the lower Rhaetian. These observations suggest a rather slow temporal diversification of the first coccolithophorids.
□ *Zlambach, Prinsiosphaera triassica, Crucirhabdus, Archaeozygodiscus, Eoconusphaera*

Isaline Demangel ✉ [isaline.demangel@geol.lu.se], Institute of Earth Sciences, University of Graz, NAWI Graz Geocenter, Graz, Austria, Department of Geology, University of Lund, Lund, Sweden; Zsófia Kovács [zsofia.kovacs@geol.lu.se], Institute of Earth Sciences, University of Graz, NAWI Graz Geocenter, Graz, Austria, Department of Geology, University of Lund, Lund, Sweden; Silvia Gardin [silvia.gardin@upmc.fr], Centre de Recherche sur la Paléobiodiversité et les Paléoenvironnements, Sorbonne Université, Paris, France; Leopold Krystyn [leopold.krystyn@univie.ac.at], Department of Palaeontology, University of Vienna, Althanstrasse 14, 1090 Vienna, Austria; Werner E. Piller [werner.piller@uni-graz.at], Institute of Earth Sciences, University of Graz, NAWI Graz Geocenter, Graz, Austria; Andre Baldermann [baldermann@tugraz.at], Institute of Applied Geosciences, Graz University of Technology, NAWI Graz Geocenter, Rechbauerstrasse 12, 8010 Graz, Austria; Sylvain Richoz [sylvain.richoz@geol.lu.se], Institute of Earth Sciences, University of Graz, NAWI Graz Geocenter, Graz, Austria, Department of Geology, University of Lund, Lund, Sweden; *manuscript received on 23/04/2022; manuscript accepted on 04/11/2022; manuscript published on 21/02/2023 in* Lethaia 56(1).

The Late Triassic is a key interval for calcareous nannofossil evolution, to understand their subsequent expansion in the oceans and their importance in present-day marine ecosystems. This period records the First Occurrence (FO) of calcareous nannofossils in the Carnian, their early evolution in the Rhaetian and their near-extinction at the Triassic/Jurassic boundary. Investigations on the oldest calcareous nannofossils are numerous (e.g. Prins 1969; Deflandre 1970; Di Nocera & Scandone 1977; Moshkovitz 1982; Jafar 1983; Bown 1985, 1987; Janofske 1987, 1992; Posch & Stradner 1987; Bralower *et al.* 1991; Bellanca *et al.* 1993; Erba 2006; Gardin *et al.* 2012; Preto *et al.* 2013; Demangel *et al.* 2020) and have allowed tracing of the FO back to the Carnian with the occurrence of three calcispheres, *Obliquipithonella prasina* (Janofske 1992), *Orthopithonella misurinae* (Janofske 1992) and *Carnicalyxia tabellata* (Janofske 1992).

https://doi.org/10.18261/let.56.1.5

The most abundant Triassic calcareous nannofossil, *Prinsiosphaera triassica triassica* (Fischer *et al.* 1967) (nannolith), and the coccolithophorids appeared in the middle Norian, followed by the occurrence of the Eoconusphaeraceae (nannolith) in the lower Rhaetian (Demangel *et al.* 2020). Attention was given to the end-Triassic, recording one of the 'Big-Five' extinctions just before the Triassic/Jurassic boundary (e.g. Clémence *et al.* 2010; Preto *et al.* 2012; Bottini *et al.* 2016). During this event, the red-plastid containing lineages, dinoflagellates, nannoliths (Eoconusphaeraceae, *P. triassica triassica*) and coccolithophorids experienced high extinction rates (Richoz *et al.* 2012). However, in between their occurrence (Carnian to the lower Rhaetian) and the end-Triassic event (upper Rhaetian – *Choristoceras marshi* Zone), the evolution of the early calcareous nannofossils is poorly investigated. Preto *et al.* (2013) have presented a quantification of the most abundant species, *P. t. triassica,* in two Tethyan basins in Central and South Italy: They contribute 0 to 10% of the total rock volume during the Norian, 20 to 40% in the middle Rhaetian and up to 60% in the late Rhaetian in more proximal settings and between 0 to 20% in more distal settings. On the contrary, Demangel et al. (2020) have presented a quantification at Steinbergkogel in the Austrian Northern Calcareous Alps (NCA) where *P. t. triassica* account for 0 to 2% of the total rock volume during the Norian and for 2 to 4% during the lowermost Rhaetian in distal settings.

To document the missing information on the early evolution of the calcareous nannofossils, this study focuses on the *Paracochloceras suessi* and *Vandaites stuerzenbaumi* ammonoid Zones, covering the lower and middle Rhaetian (see Galbrun et al. 2020) of the Zlambach section (Austria – Northern Calcareous Alps). The impact of diagenesis on the preservation of the nannofossils record was investigated based on trace element content using Inductively Coupled Plasma-Optical Emission Spectrometry (ICP-OES) measurements. Scanning Electron Microscopy (SEM) and Light Microscopy (LM) were used to obtain qualitative and quantitative estimates of the abundance and temporal evolution of the lower to middle Rhaetian calcareous nannofossils.

Geological setting

During the Rhaetian (208.50–201.36 Myr; Galbrun et al. 2020), the Austrian NCA were located at a palaeo-latitude around 25° N (Gallet et al. 1996), on the western margin of the Neo-Tethys Ocean (Fig. 1). Along with the opening of the Neo-Tethys Ocean, this region was characterized by the development of widespread carbonate platform systems during the Middle and Late Triassic (Mandl 2000; Richoz & Krystyn 2015). The Dachstein carbonate platform has spread from the late Carnian until the middle Rhaetian (Krystyn *et al.* 2009). During the middle Rhaetian, parts of the platform rim deepened and subsequently changed into a basinal setting before an increase of the terrigenous influx occurred, marking the shift back to more proximal sedimentation in the late-middle Rhaetian (Kovács *et al.* 2020).

The Zlambach Formation was deposited in a toe-of-slope to open-marine basin environment and represents the interspace between the Dachstein platform and the Hallstatt basin composed of grey cherty limestones of the Carnian Pötschen Formation overlain by the Rhaetian Zlambach Formation (Fig. 1). This formation comprises here alternations of autochthonous, bioturbated marlstones and subordinate marly micritic limestones of greyish colour with episodically embedded fine-grained calciturbidites of allochthonous origin and other mud/debris flows (Matzner 1986; Krystyn 1987, 1991; Richoz et al. 2012; Richoz & Krystyn 2015; Galbrun et al. 2020) (Fig. 2). The allodapic limestone beds appear as grainstones to packstones with stylolites at the layer boundaries (Matzner 1986) and contain common reworked reefal debris (Richoz & Krystyn 2015). The autochthonous sedimentary rocks contain some ostracodes, radiolarians and ammonoids including *Paracochloceras suessi, Vandaites stuerzenbaumi* and *Choristoceras* marshi. The ammonoids are used in parallel with rare conodonts and foraminifera for biostratigraphical correlation (Piller 1978; Matzner 1986; Richoz & Krystyn 2015; Galbrun *et al.* 2020). Some marlstone horizons are rich in redeposited corals (Frech 1890), non-segmented calcareous sponges, spongiomorphs, hydrozoans, solenoporaceans, bryozoans, brachiopods, echinoderms, serpulids, ostracodes and diverse foraminifera fauna (Kristan-Tollmann 1964; Piller 1978). Additionally, abundant pollen and spores are recognizable throughout the entire Zlambach Formation (Krystyn & Kuerschner 2005), which is at least 150 m thick.

Material and methods

The studied section, the Kleiner Zlambach, represents a 55-m-thick profile, which covers the lower part of the Zlambach Formation, i.e., the *P. suessi* and *V. stuerzenbaumi* Zones (Fig. 2), until the base of the *C. marshi* Zone. The remaining part of the last zone is covered at this outcrop. The Kleiner Zlambach section is located

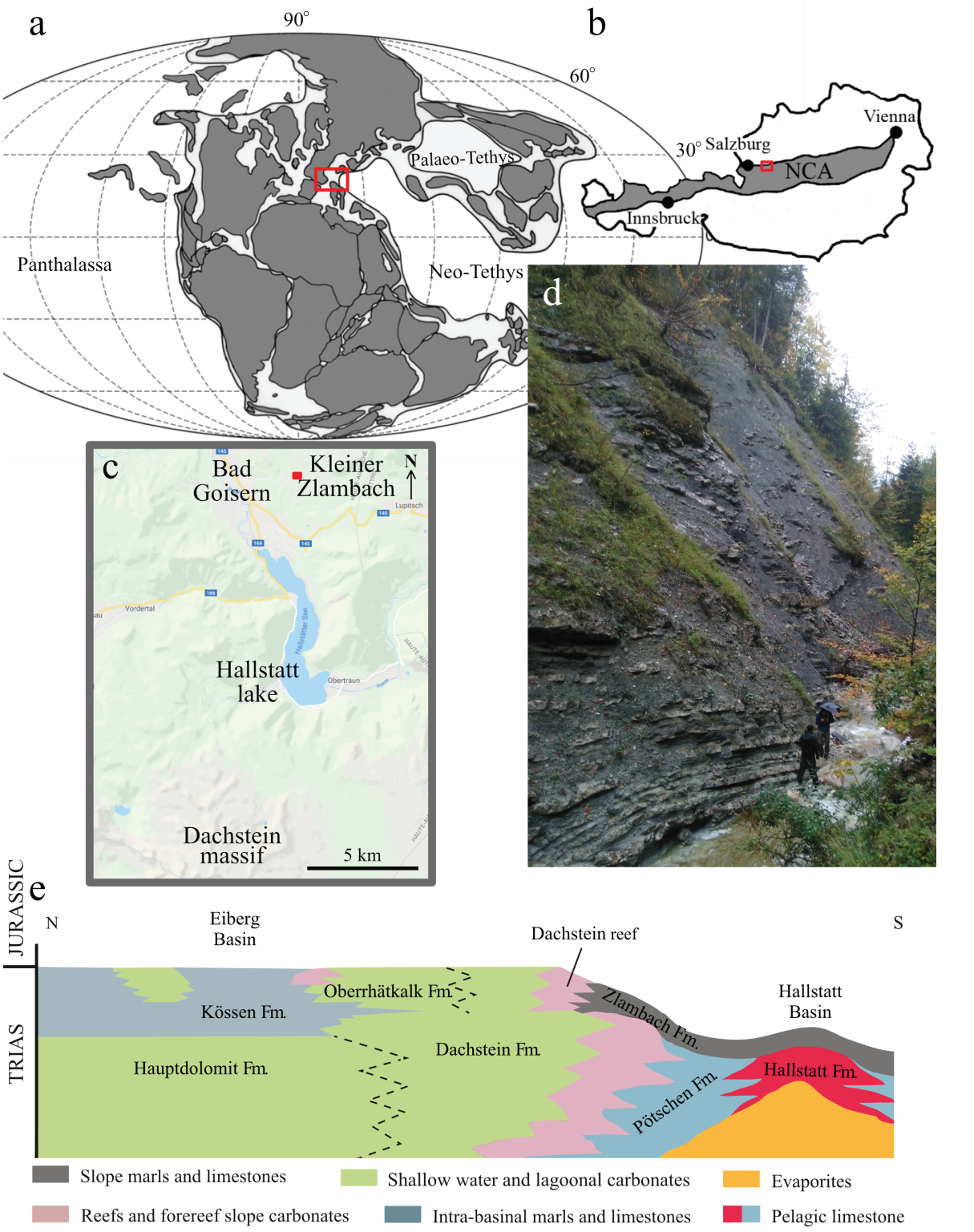

Fig. 1. Location and stratigraphy of the studied section at Kleiner Zlambach, Austria, Northern Calcareous Alps (NCA). A, global palaeogeographical reconstruction during the Late Triassic with the NCA (red square) located at the western Neo-Tethys margin (modified from Scotese 2004; Golonka 2007; Nakada *et al.* 2014). B, location of the Zlambach section (red square) in the central NCA (modified after Schorn & Neubauer 2014). C, location of the Kleiner Zlambach (red square) in the Salzkammergut region of Austria, north of the Dachstein summit and Hallstatt lake and near the village Bad Goisern. D, outcrop at the Kleiner Zlambach section (people for scale are ca. 1.80 m tall). The base of the section shown here is at 40 m on the section log (Fig. 2). E, schematic stratigraphy of the Austrian Northern Calcareous Alps during the Late Triassic (after Mandl 2000).

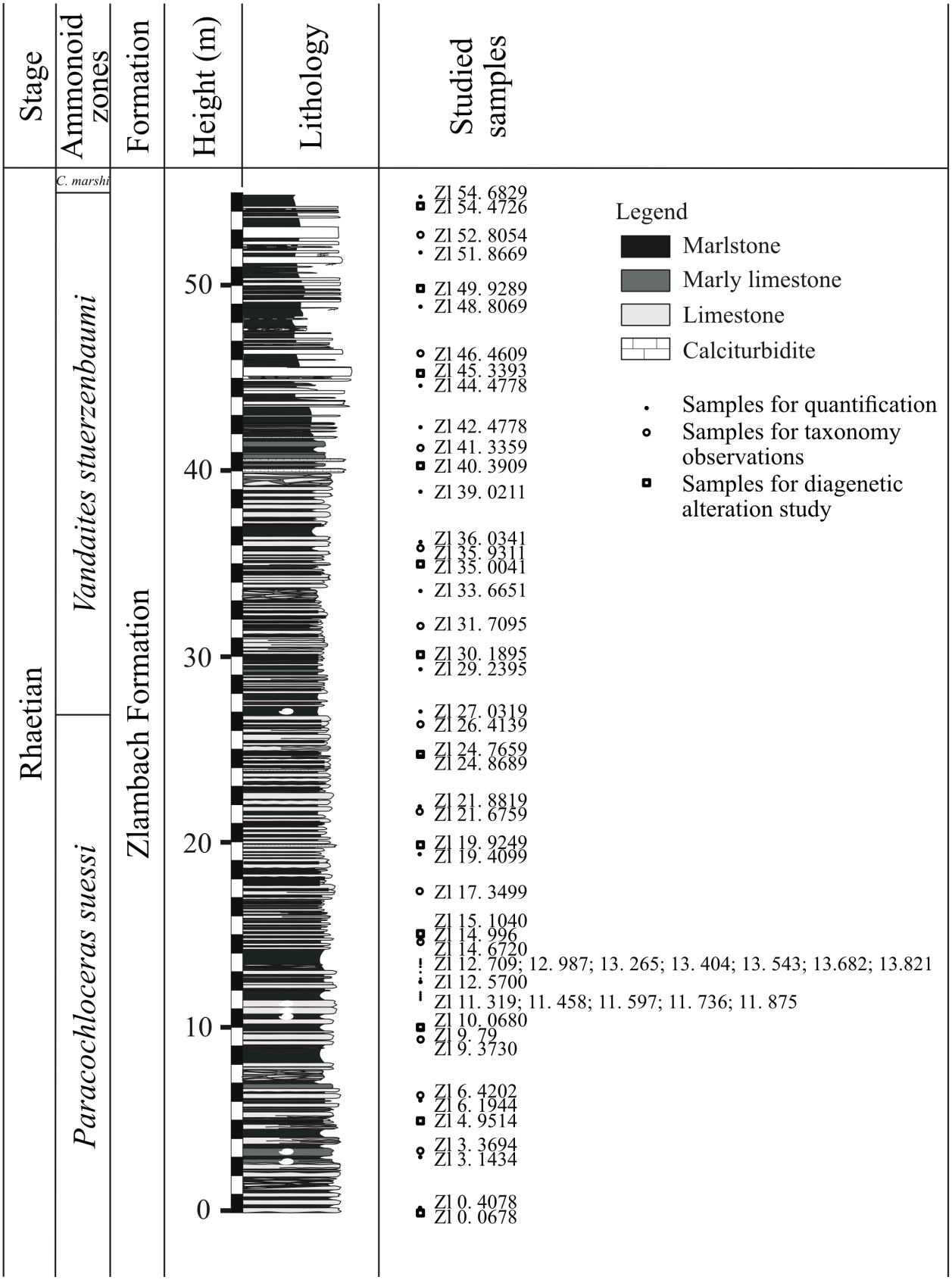

Fig. 2. Lithology and biostratigraphy of the Rhaetian Zlambach Formation with ammonoid zones and position of the studied samples.

in the Austrian NCA at around 870 m altitude, about 3 km north of the Hallstatt lake and 2 km east of the village Bad Goisern along the Kleiner Zlambach river (coordinates: 47.642278, 13.659267) (Fig. 2).

Sampling and nannofossil quantification

A total of 31 samples (Fig. 2) were prepared following the smear slide preparation technique of Bordiga *et al.* (2015). The bulk rock samples were gently disintegrated by scratching the freshly prepared rock surfaces, then 0.05 g of dried, pulverized materials were mingled with 50 mL of a buffered ammonia solution. Using a micropipette, 1500 µL of the suspensions were transferred to coverslips and left to dry at a temperature below 50° C to avoid aggregation of sediment particles and nannofossils. The preparations were mounted on standard glass slides using Norland Optical Adhesive and dried with an UV lamp. The samples are named according to their positions in metres along the studied profile (Fig. 2).

The samples were observed using an Olympus BX50 light microscope at a magnification of x2500. Two transects taken along the short axis (24 mm) of each slide were quantified, one at the middle and one at ¼ of the extremity. The average of both transects was considered for the calculation of the relative and absolute abundances. All the species present in the studied samples were quantified. The relative abundances of each species were calculated considering the entire nannofossil assemblage. The 95% confidence interval for the relative abundance was calculated based on Clopper & Pearson's (1934) method, following the instruction of Suchéras-Marx *et al.* (2019a) using the free statistical software PAST (Hammer *et al.* 2001). The absolute abundance of nannofossils per gram of bulk sediment (Nanno/g) was calculated for each species and obtained following the equation developed in Bordiga *et al.* (2015):

$$X = (Nanno \times A) \div (f \times n \times W) \qquad \text{(equation 1)}$$

where X is the absolute nannofossil abundance per gram of sediment (Nanno/g), *Nanno* is the average number of nannofossil counted on the two transects per sample, A is the area of the coverslip (768 mm^2), f is the area of one field of view (FOV: 0.0078 mm^2), n is the number of FOVs counted (240) and W is the weight of dry sediment placed on the coverslip (g) after dilution.

The nannofossils accumulation rate was calculated following the equation 2 (modified from Suchéras-Marx *et al.* 2014):

$$\text{Nannofossils accumulation rate (nannofossils / } m^2 \text{ / yr)} = X \times \text{sedimentation rate} \times \rho_{\text{sediment}} \qquad \text{(equation 2)}$$

where X is the absolute nannofossils abundance (Nanno/g) calculated via equation 1. The bulk accumulation rate considered here is 15.97 m / Myr, as estimated by Galbrun *et al.* (2020) using cyclostratigraphy for the Zlambach Formation. The rate is considered to be linear as similar values have been obtained over the duration of the *P. suessi* Zone (1.83 Myr) and *V. stuerzenbaumi* Zone (1.63 Myr) and is verified further by the identical number of 405 000 years cycles in each ammonoid zone (Galbrun *et al.* 2020). ρ_{sediment} corresponds to the measured rock density obtained from 25 samples including nineteen on small pieces of rocks for each quantified sample and six on larger rocks (around one kilogramme) to control the density obtained on small pieces. The density ranges from 1.8 to 3.2 g/cm^3 with an average for both set of rocks of 2.4 g/cm^3. For the limestones, the density was calculated following the basic method of mass per rock volume measurements. For marlstones and marly limestones, the density was calculated using the respective sample mass divided by the difference of the sample mass to water mass in a known water volume, before and after immersion of the sample.

To ensure direct comparison with the results of the Upper Triassic Italian sections reported by Preto *et al.* (2013) and to understand the contribution to carbonate deposition of the main calcifier, the percentage of *P. t. triassica* in the sediment (wt% $CaCO_{3P.\ t.\ triassica}$) was calculated with equations 3 and 4. Therefore, the volume of all *P. t. triassica* (cm^3) was determined following equation 3. Several specimens with entire diameter visible were measured for each sample and the corresponding mean radius were included in equation 3 to consider the size variation through the studied succession. The use of the mean radius introduces a minor inaccuracy; therefore, the standard error of the mean was computed (ranging: 0.08 to 0.27) and integrated into the error bars (1 σ) of the wt% $CaCO_{3P.\ t.\ triassica}$. The mass of the total volume of *P. t. triassica* (g $CaCO_3$) was computed following equation 4. The density of the test was assumed to be 2.7 g/cm^3 referring to the calcite mineralogy of *P. t. triassica* specimens (Young & Ziveri 2000).

$$V_{P.\ t.\ triassica} = \frac{4}{3\pi r^3} \times X \qquad \text{(equation 3)}$$

$$M_{P.\ t.\ triassica} = V_{P.\ t.\ triassica} \times \rho_{\text{calcite}} \qquad \text{(equation 4)}$$

The carbonate palaeoflux associated with the main Upper Triassic calcifier abundance, *P. t. triassica* (g $CaCO_3/m^2/yr$), was calculated using the mass of *P. t. triassica* (g $CaCO_3$) from equation 4 and considering the sedimentation rate and density as indicated before.

SEM sample preparation

Twelve samples were prepared for a Scanning Electron Microscopy (SEM) study to observe morphological details and to evaluate possible size changes of the calcareous nannofossils over time. The method described in Demangel *et al*. (2020) was followed, i.e., the samples were cut in blocks with a surface of 1 cm^2 and then polished with 600 and 1200 diamonds discs using deionized water. The blocks were etched for 15 seconds in 0.1% HCl solution and cleaned for 7 seconds in an ultrasonic bath with distilled water. The samples were dried overnight at 50°C and finally coated with 1 nm of platinum/palladium using a Cressington Sputter Coater 208HR. The SEM analyses were done with a TESCAN MIRA 3 electron microscope at Lund University.

Diagenetic study

The degree of diagenetic alteration of the samples was estimated based on common enrichment or depletion trends of major and minor elements (Na, Sr, Fe, Mn, etc.) recorded in the carbonate fraction obtained with inductively coupled plasma optical emission spectroscopy (Brand & Veizer 1980; Baldermann *et al*. 2020). A total of 12 samples was analysed across the entire sections with a vertical resolution between 5 to 6 m. Acid digestion of the carbonate fraction (including dolomite) was carried out by reacting 0.050 g of the powdered sample with 5 drops of 6% HNO_3 of suprapure grade and 50 mL of 2% HNO_3 for 12 h at 80°C. Afterwards, the acid-soluble fraction was separated by filtration through a 0.45 µm cellulose acetate membrane. Chemical analyses were carried out on a Perkin Elmer OPTIMA 8300 at the Institute of Applied Geosciences, Graz University of Technology, to obtain the total aqueous concentrations of Al, Ba, Ca, Cd, Co, Cr, Cu, Fe, K, Li, Mg, Mn, Na, Ni, Si, Sr and Zn in each sample. The analytical precision (2σ, 3 replicates) is better than ± 3% for all elements, as determined by replicate analyses of NIST 1640a, in-house and SPS-SW2 Batch 130 standards (Baldermann *et al*. 2018 a, b).

Results

The Rhaetian calcareous nannofossil assemblage, Zlambach section

The Rhaetian interval at the Zlambach section presents almost all of the Upper Triassic calcareous nannofossils known so far. The Prinsiosphaeraceae are present with two taxa, *Prinsiosphaera triassica triassica* (Fig. 3) and *P. triassica crenulata* (Jafar 1983; Fig. 4). Two conical forms are present with *Eoconusphaera hallstattensis* (Demangel et al. 2021; Fig. 5) and then *Eoconusphaera zlambachensis* (Moshkovitz 1982; Fig. 6). Three calcispheres, probably related to the Dinophyceae were observed, including *Orthopithonella geometrica* (Jafar 1983; Fig. 7A), *Obliquipithonella rhombica* (Janofske 1987; synonymous to *Pirumella rhombica*; Fig. 7B) and *Thoracosphaera wombatensis* (Bralower *et al*. 1991; Fig. 7C). The coccolithophorids are present with *Crucirhabdus minutus* (Jafar 1983; Fig. 8A), *Archaeozygodiscus koessenensis* (Bown 1985; Fig. 8B) and *C. primulus* (Prins 1969; Fig. 8C). Additionally, one coccolith-like specimen was observed but not identified at the species level (Fig. 9). Finally, the nannolith *Carnicalyxia tabellata* is barely observable, whereas *Cassianospica curvata* (Janofske 1992) and *Hayococcus floralis* (Jafar 1983) were not observed in this study, even though they were observed in time-equivalent Rhaetian sediments at other localities (e.g. Bralower *et al*. 1991; Janofske 1992; Bown & Cooper 1998; Bottini *et al*. 2016).

Along the section, *P. t. triassica* was observed in a good preservation state. Mainly, *P. t. triassica* appears intact or broken in half with the outer and inner part being composed of randomly oriented groups of parallel-oriented, thin tabular, rhombohedral calcite crystals (Fig. 3). In sample Zl 42, 4778 some specimens of *P. triassica crenulata* also occur, consisting of groups of parallel-oriented, thin tabular, rhombohedral calcite crystals, which appear as striation (Fig. 4).

The Eoconusphaeraceae family is present throughout the Zlambach section. Two different species were observed with dominance at two specific intervals: *E. hallstattensis* (Fig. 5) is present from the base of the section (*Paracochloceras suessi* Zone – lower Rhaetian) to sample Zl 29. 2395 (*Vandaites stuerzenbaumi* Zone – middle Rhaetian). Above, *E. zlambachensis* (Fig. 6) appears and dominates from sample Zl 33. 6651 (*Vandaites stuerzenbaumi* Zone – middle Rhaetian) until the top of the section, with the persisting presence of a few *E. hallstattensis* specimens after the transition.

Calcispheres (other than *P. t. triassica*) are present in almost all of the samples, except for the interval between 11.3 and 11.7 m and at 12.9 m, but sometimes they are represented by only one or two species. Among the three species identified, *Obliquipithonella rhombica* (Fig. 7B) is the most abundant (present in 21 out of 31 samples), followed by *Orthopithonella geometrica* (Fig. 7A) and *Thoracosphaera wombatensis* (Fig. 7C). The three species do not vary in shape across the investigated

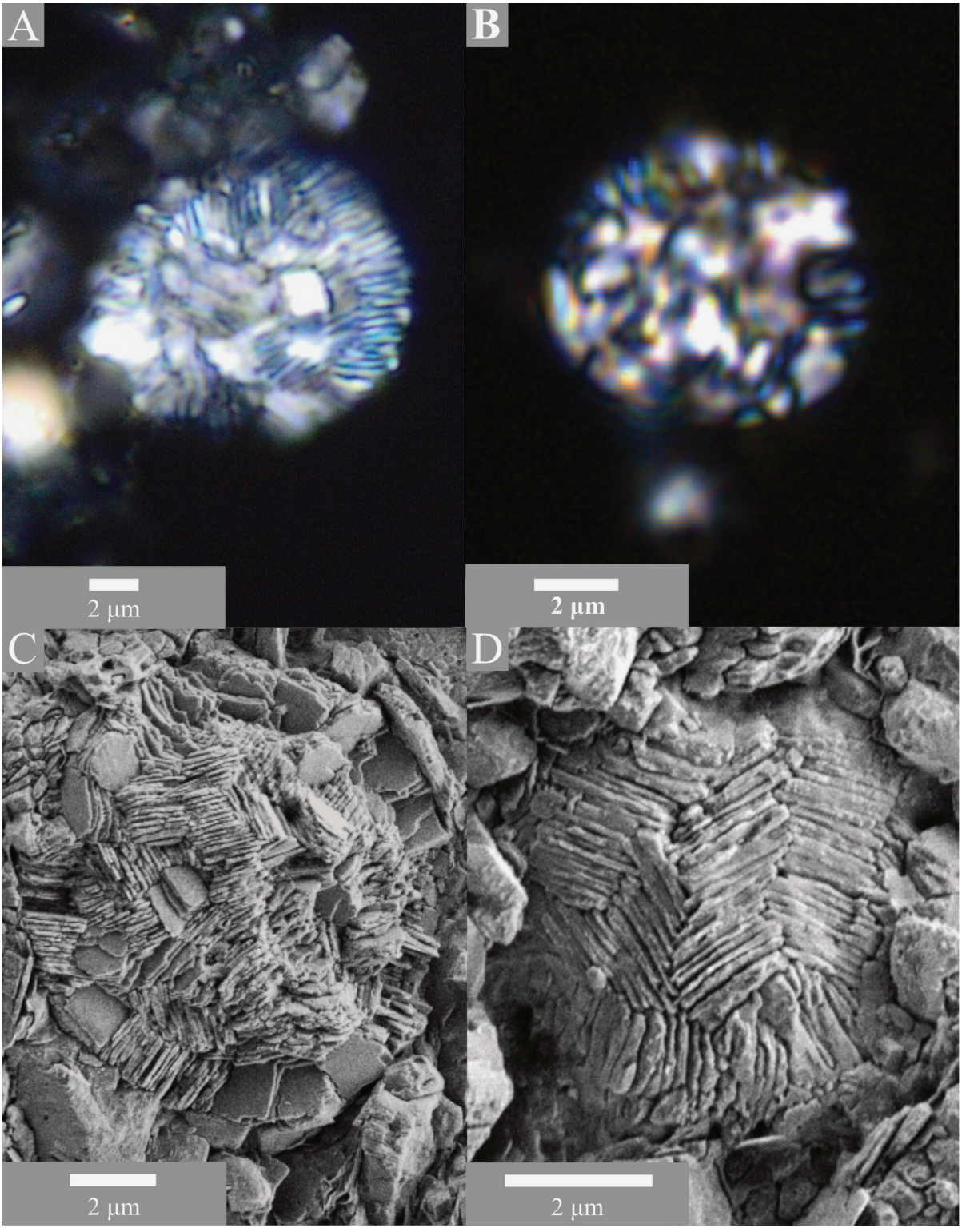

Fig. 3. Prinsiosphaera triassica triassica in LM with XPL (A, B) and similar specimens under the SEM (C, D). The inner part of the calcisphere is well-preserved and composed of groups of calcite lamellae. Within each group, the lamellae are stacked parallel to each other. Between groups, the orientation appears random. Specimens are from the lower Rhaetian, corresponding to samples: Zl 5.5164 (A, B) and ZL 6.4202 (C, D).

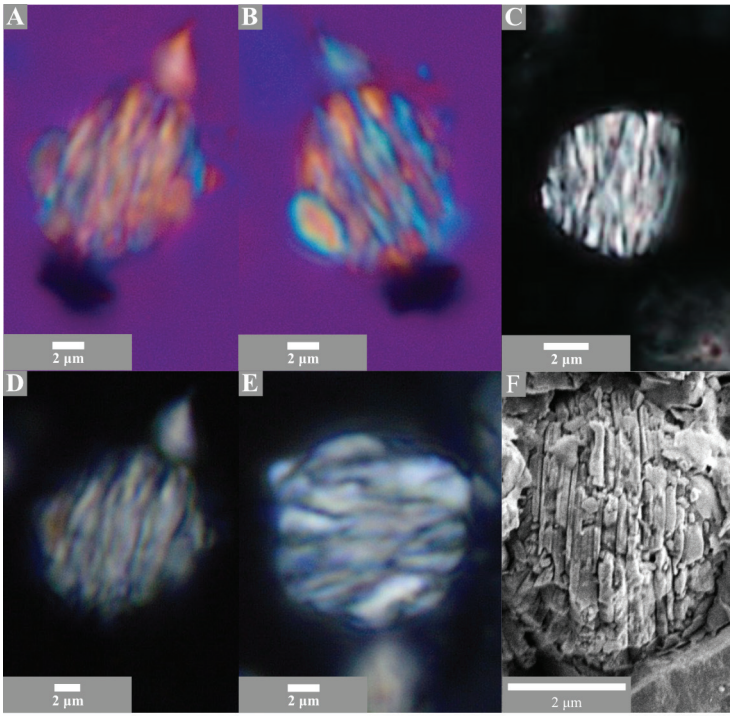

Fig. 4. *Prinsiosphaera triassica crenulata* (Jafar 1983) in LM (A – E) with XPL and gypsum plate (A, B) and under the SEM (F). Specimens show calcite lamellae organized in stripes and are from the middle Rhaetian, corresponding to sample ZL 52.8554.

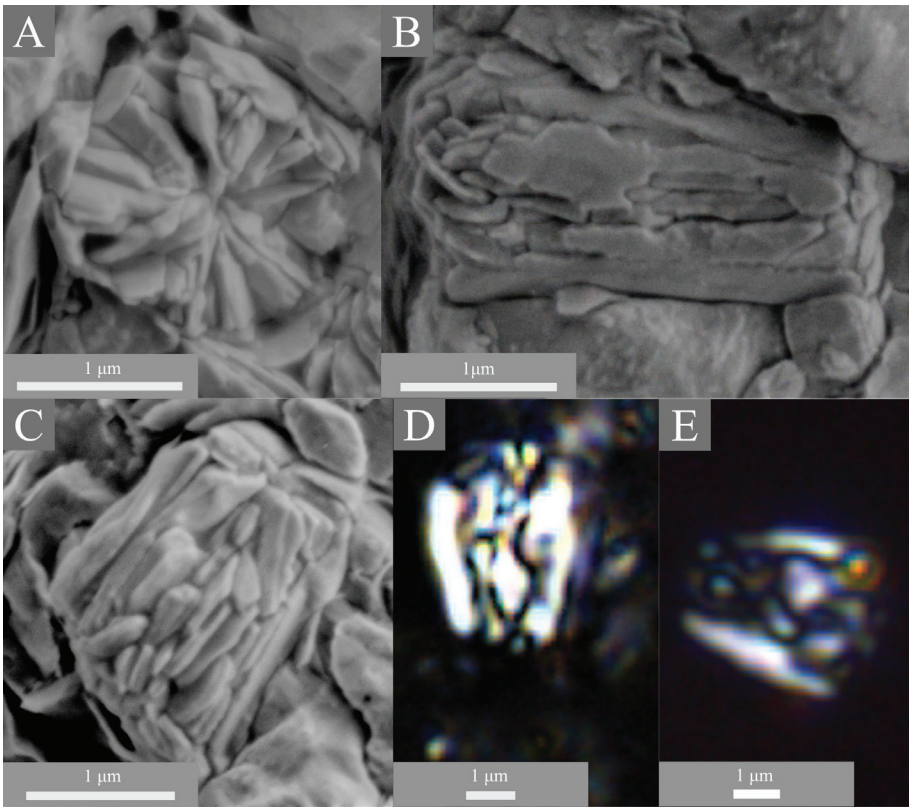

Fig. 5. *Eoconusphaera hallstattensis* observed under the SEM (A – C; sample Zl 6.4202) and in LM with XPL (D, E). A, top view. B, side view showing the external and internal lamellae. C, side/top view showing the inner part with vertical lamellae. D, side view showing the dome shape at the distal (broader) extremity of the specimen (Zl 14.9960). E, side view (Zl 5.5164).

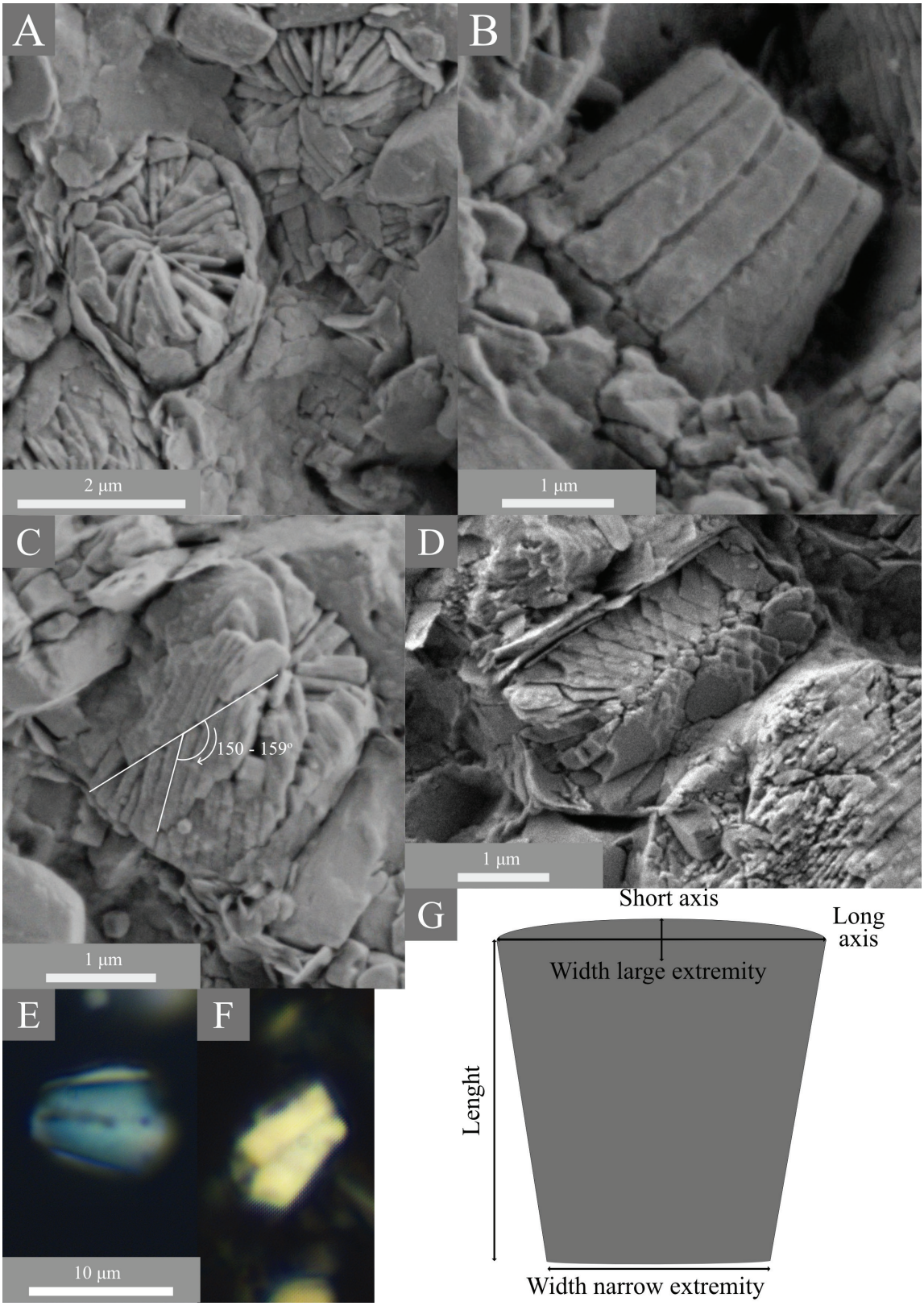

Fig. 6. Eoconusphaera zlambachensis under the SEM (A–D) and in LM (E, F). A, top view of two specimens (Zl 51.8669). B, side view showing the external lamellae (Zl 51.8669). C, side/top view showing the rows of oblique lamellae (Zl 51.8669). D, side view showing the central suture, the oblique lamellae and the external lamellae (Zl 52.8554). E, F, side view of two specimens observed in two different extinction pattern (Zl 54.6829). G, schematic view showing the measurements done on the Eoconusphaeraceae.

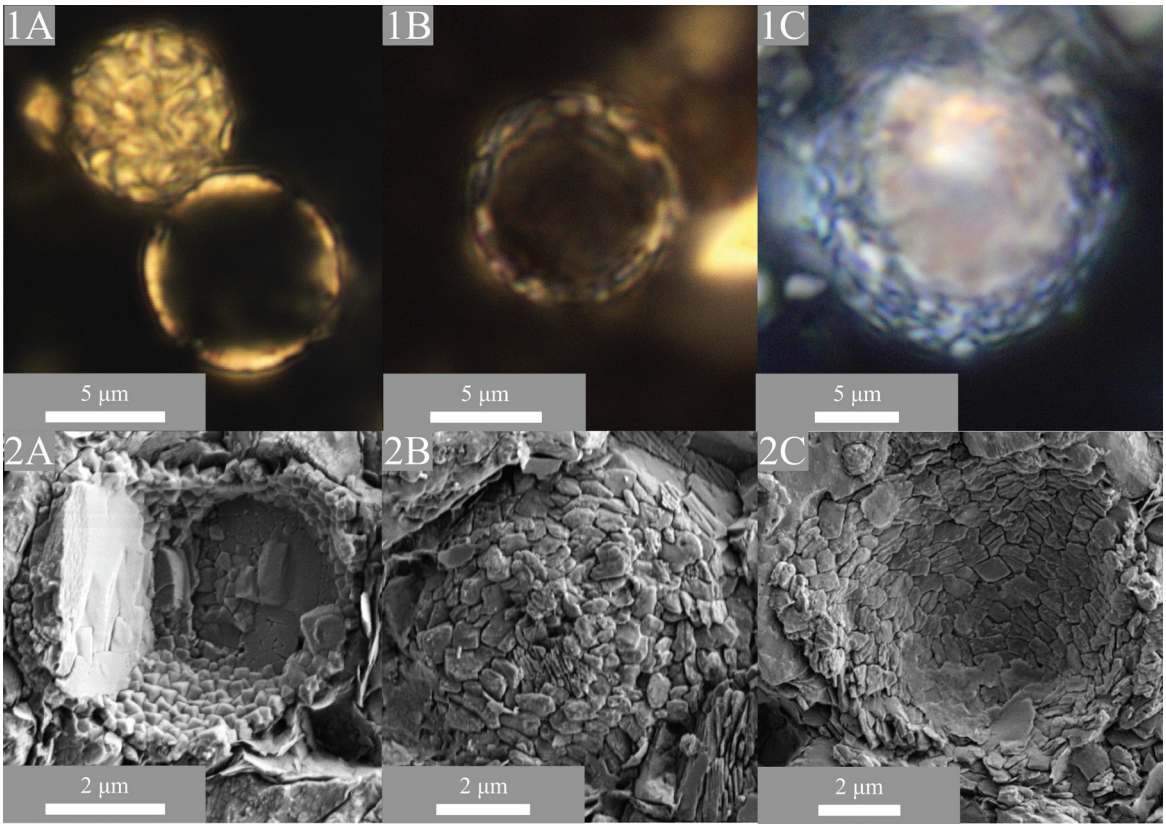

Fig. 7. Calcispheres under LM with XPL (1; Zl 39.0211) and SEM (2). A, *Orthopithonella geometrica* (lower Rhaetian; Zl 6.4202, 2A). B, *Obliquipithonella rhombica* (lower Rhaetian; Zl 52.8554, 2B). C, *Thoracosphaera wombatensis* (middle Rhaetian; Zl 52.8554, 2C).

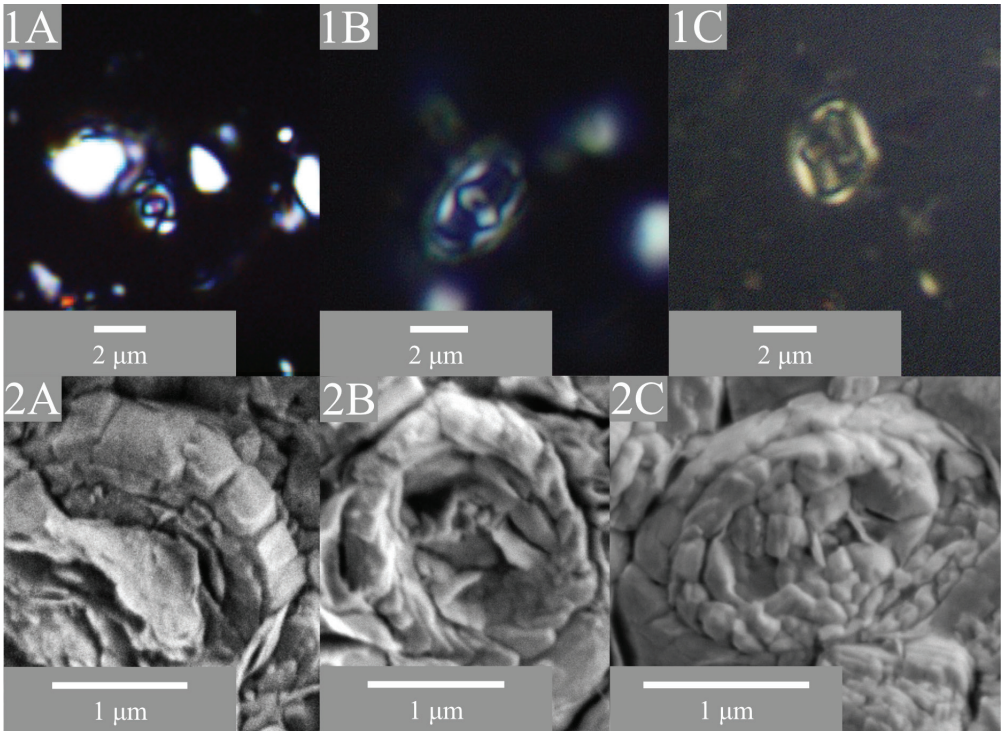

Fig. 8. Coccoliths in LM with XPL (1) and under SEM from sample Zl 6.4202 (2). A, *Crucirhabdus minutus* (lower Rhaetian; Zl 5.5164, 1A). B, *Archaeozygodiscus koessenensis* (lower Rhaetian; Zl 8.6847, 1B). C, *Crucirhabdus primulus* (lower Rhaetian; Zl 14.9960, 1C).

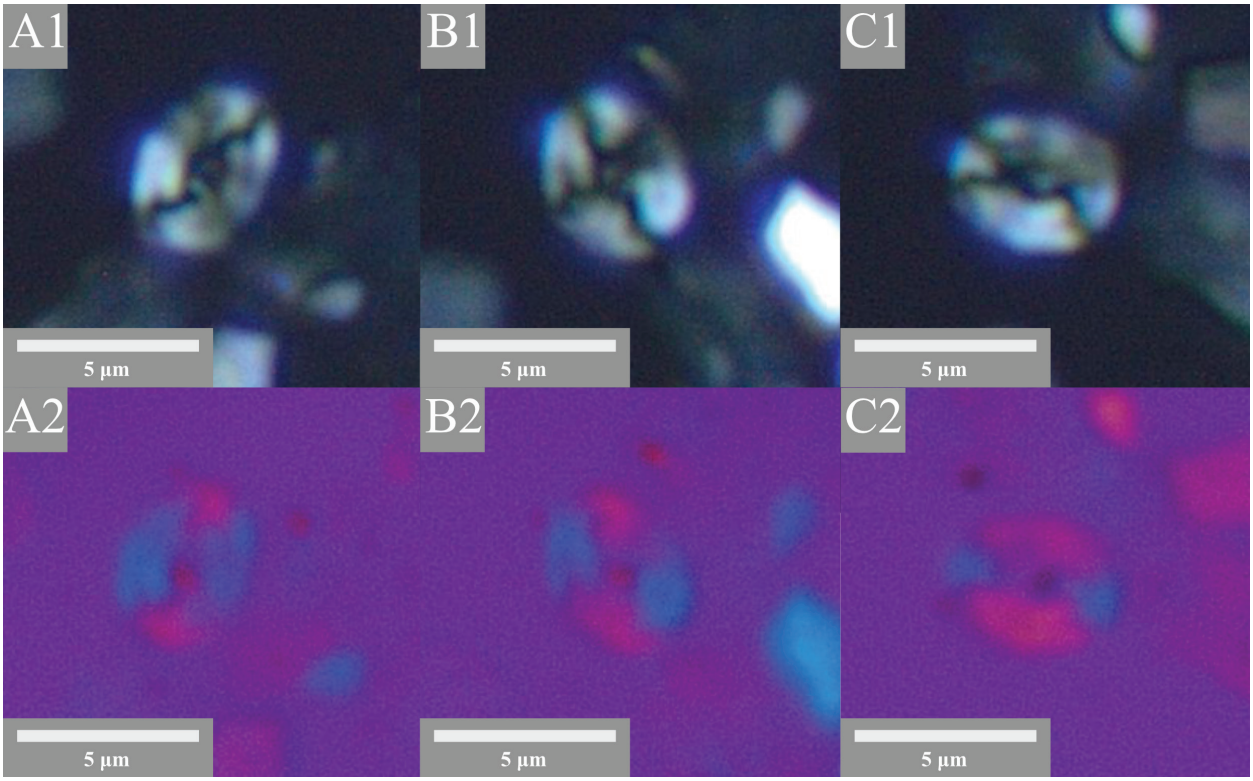

Fig. 9. Specimen of an unknown coccolith, sample Zl 6.1944 from the Lower Rhaetian in LM with XPL (1) and gypsum plate (2).

section. The mean sizes of *Thoracosphaera wombatensis* (N = 4), *Orthopithonella geometrica* (N = 6) and *Obliquipithonella rhombica* (N = 2) are 7 (± 2) µm, 8 (± 2) µm and 9 µm, respectively.

Coccolithophorids are present in every sample, except for sample Zl 13.682, however, some specimens remain undetermined at the species level due to lack of characteristic structures. The three coccolithophorid species do not vary in shape and size during the Rhaetian: *C. minutus* and *C. primulus* have a mean size of 2.4 µm × 1.7 µm and *A. koessenensis* has a mean size of 3 µm × 2 µm, out of four specimens measured for each species.

A possible coccolith was observed in sample Zl 6.1944. It has an oval shape, a length of 5 µm and a width of 4 µm and presents an oval, opened, central area that is likely filled by a central spine visible as knobs under the LM. With polarized light, it shows a weakly birefringent rim with kinked isogyres (Fig. 9). Its structure differs from Upper Triassic heterococcoliths, which are murolith presenting narrow, bicyclic rims with an outer cycle made of V-units. However, this specimen (Fig. 9) seems to have a narrow central area and a wide rim similar to a placolith presenting a well developed R-unit rim (e.g. *Watznaueriaceae*). Alternatively, the structure can be related to a holococcolith such as *calculites* presenting a proximal plate of four blocks, a central spine and appears entirely bright in cross polarized light. Only one specimen has been observed under the light microscope so far, and more investigation is needed to prove if it is a real component of the coccolith assemblage or an artefact, although contamination is a lower risk since the smear slides were prepared in a clean room with the samples from the Zlambach section only.

Calcareous nannofossil abundance

The nannofossil assemblage is mostly dominated by the calcisphere *P. t. triassica* (Fig. 3) with relative abundances between 30 and 88% (Fig. 10), while the other subspecies *P. triassica crenulata* (Fig. 4) is present in low abundance. The conical nannolith, *Eoconusphaera hallstattensis* (Fig. 5) and *Eoconusphaera zlambachensis* (Fig. 6), show relative abundances between 5 and 67% (Fig. 10). In five samples (out of 19 samples), they are even more abundant than *P. t. triassica*. The other calcispheres (*P. t. triassica* not included), *Orthopithonella geometrica* (Fig. 7A), *Obliquipithonella rhombica* (Fig. 7B) and *Thoracosphaera wombatensis* (Fig. 7C), display relative abundances between 0.1 and 33% if present in the sample (Fig. 10). Throughout the section, the dominant species, i.e., *Obliquipithonella rhombica,* shows an abundance between 1 and 32 specimens per transect, reaching the maximum in sample Zl 42.4778.

Orthopithonella geometrica is present in many samples (20 of 31). The abundance of this species varies between 1 and 15 specimens per transect with its maximum in sample Zl 13.682. *Thoracosphaera wombatensis* is present in 15 out of 31 samples with a low abundance between 1 and 9 specimens per transect, reaching its maximum in sample Zl 42.4778. The three coccolithophorids, *Crucirhabdus minutus* (Fig. 8A), *Archaeozygodiscus koessenensis* (Fig. 8B) and *Crucirhabdus primulus* (Fig. 8C), represent a minor part of the total nannofossils assemblage with relative abundances between 0.2 and 8%, if present (Fig. 10). *Crucirhabdus minutus* dominates the coccolithophorids assemblage, followed by the total of specimens not identified at the species level, then by *C. primulus* and *A. koessenensis*. *C. minutus* is present in most of the samples (23 of 31) reaching a maximum abundance during the *V. stuerzenbaumi* Zone, with 51 specimens per transect at 36 m. *Crucirhabdus primulus* was observed in 19 samples (of 31), with two slight increases in abundance, reaching 5 and 10 specimens per transect at 9.8 and 36 m, respectively. *A. koessenensis* is scarce in the lower to middle Rhaetian and was found only in 10 samples (of 31). This species reaches a maximum of 3 to 4 specimens per transect in the middle Rhaetian between 36 and 42.5 m in the section. The same trends in abundance were recognized for the undetermined specimens with 1 and 9 specimens per transect along the section and two increases reaching 20 and 28 specimens per transect at 9.8 and 36 m in the profile, respectively (Fig. 11).

The absolute abundances of each species present in the assemblage are represented in Figure 11. The nannofossil accumulation rate varies around 8×10^9 (nannos / m^2 / yr) (Fig. 10). The nannofossil accumulation rate increases toward 10 m, reaching 9×10^9 (nannos / m^2 / yr). After a slight decrease, the value increases again to around 20 m to 1×10^{10} (nannos / m^2 / yr). Minimum values are around 30 m in the profile with 8×10^8 (nannos / m^2 / yr). The maximum nannofossil accumulation rate is reached at 36 m with 3.5×10^{10} (nannos / m^2 / yr), followed by a decrease to 3.5×10^9 (nannos / m^2 / yr) at the top of the section.

The wt% $CaCO_{3P.\ t.\ triassica}$ varies around 4%, with fluctuation throughout the Zlambach section, however, four distinctive increases are recognizable (Fig. 10). In the *P. suessi* Zone, the percentage of *P. t. triassica* increases gradually to reach 14% from the base of the section until 10 m. Above, the values start to decrease, reaching 7.5% at around 12 m and then 1.8% at around 15 m. From 19 to 22 m, the values increase between 10 and 13%. The concentration of *P. t. triassica* decreases again afterwards, reaching a minimum of 0.5% at around 30 m. At 36 m, the maximum concentration is reached with 18%. Toward the top of the Zlambach section, the percentage decreases gradually, fluctuating between 0.8 to 7%. The carbonate flux linked to the abundance of *P. t. triassica* shows a variation between 0.02 and 6 g $CaCO_3$ per m^2 per year, however, the median value lies around 2 g $CaCO_3$ per m^2 per year. All the data are available online: 10.17632/r62z95vzn8.3.

Nannolith size variation

Prinsiosphaera triassica triassica.- The size of *P. t. triassica* in the section varies between 4 and 12 µm. The mean diameter ranges from 9 µm in the lower Rhaetian to 6 µm in the middle Rhaetian, with a marked decrease in the mean size of *P. t. triassica* at around the *P. suessi – V. stuerzenbaumi* zones boundary (Fig. 10). The *P. suessi* Zone records a broad range of *P. t. triassica* sizes, which vary from medium (5–7 µm), large (8–10 µm) and up to very large (11–13 µm), considering the size group of Clémence et al. (2010) randomly attributed. From 14 m up-section, the very large sized specimens of *P. t. triassica* disappear and within the *V. stuerzenbaumi* Zone the small sized specimens of *P. t. triassica* (< 5 µm) occur (Fig. 10).

Eoconusphaeraceae. The size variation of the two species, *E. hallstattensis* and, *E. zlambachensis*, was measured on 67 and 48 specimens, respectively, in SEM. The specimens were observed from the side view, which allows measuring of the total length and width of the distal (broad) and proximal (narrow) extremity of the truncated cone-shaped nannolith (Fig. 6G). The specimens were also observed in top view making measurements of the long and short axis of the oval-shaped extremity possible. *E. hallstattensis* has a length between 2 and 6 µm (mean = 3.5 µm), a width between 1 and 3 µm for the distal extremity (mean = 2 µm) and between 1 and 2.6 µm for the proximal extremity (mean = 1.7 µm). In the top view, *E. hallstattensis* has a long axis between 1.7 and 4.5 µm (mean = 3 µm) and a short axis between 1.3 and 3 µm (mean = 2 µm). *E. zlambachensis* has a length between 2 and 5 µm (mean = 3 µm) and a width between 1.5 and 3.5 µm for the distal extremity (mean = 2 µm) and between 1 and 2.5 µm for the proximal extremity (mean = 1.7 µm). In the top view, *E. zlambachensis* has a long axis between 2 and 3.5 µm (mean = 2.5 µm) and a short axis between 1 and 3 µm (mean = 2 µm). The inclination angle of the inner lamellae of *E. zlambachensis* (Fig. 6C) varies between 150° and 159° (based on the analysis of 17 specimens).

E. hallstattensis and *E. zlambachensis* have a broad size range across the section, but these also vary within the same sample. Their sizes range from large and small to long and narrow with all medium sizes

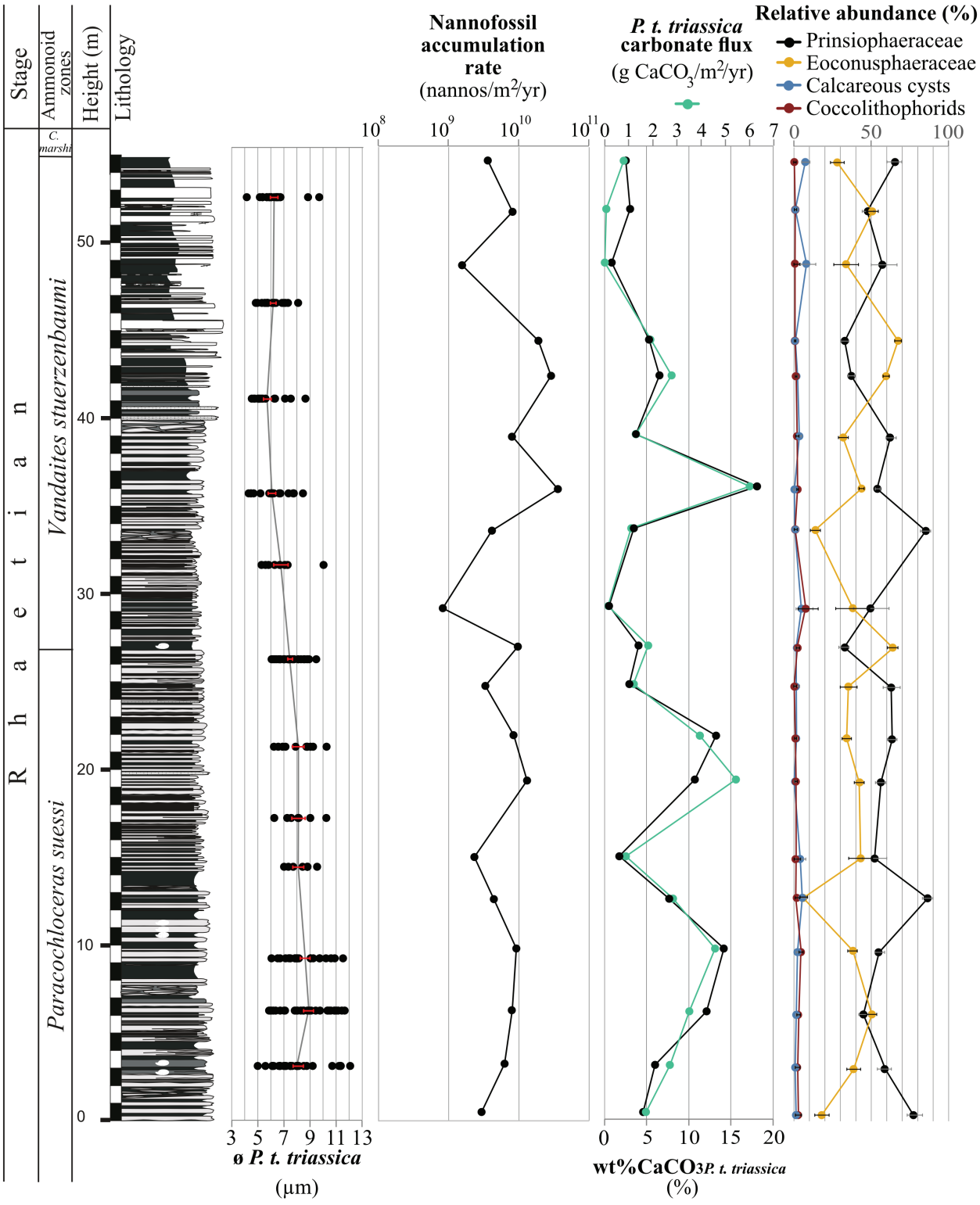

Fig. 10. Compilation of the calcareous nannofossils record at the Kleiner Zlambach section. 1st column, lithology of the Rhaetian Zlambach Formation with the P. t. triassica diameters measured for each sample (black dots) and the calculated averages (grey line) including the standard error of the mean (red error bars). 2nd column, nannofossil accumulation rate including all species present (nannos/m²/yr). 3rd column, concentration of *P. t. triassica* (%) in the sediment on the bottom axes and *P. t. triassica* carbonate flux in g of $CaCO_3$ per m² per year in the top axes. 4th column, relative abundance (%) of all calcareous nannofossils observed in the samples including the 95% confidence interval.

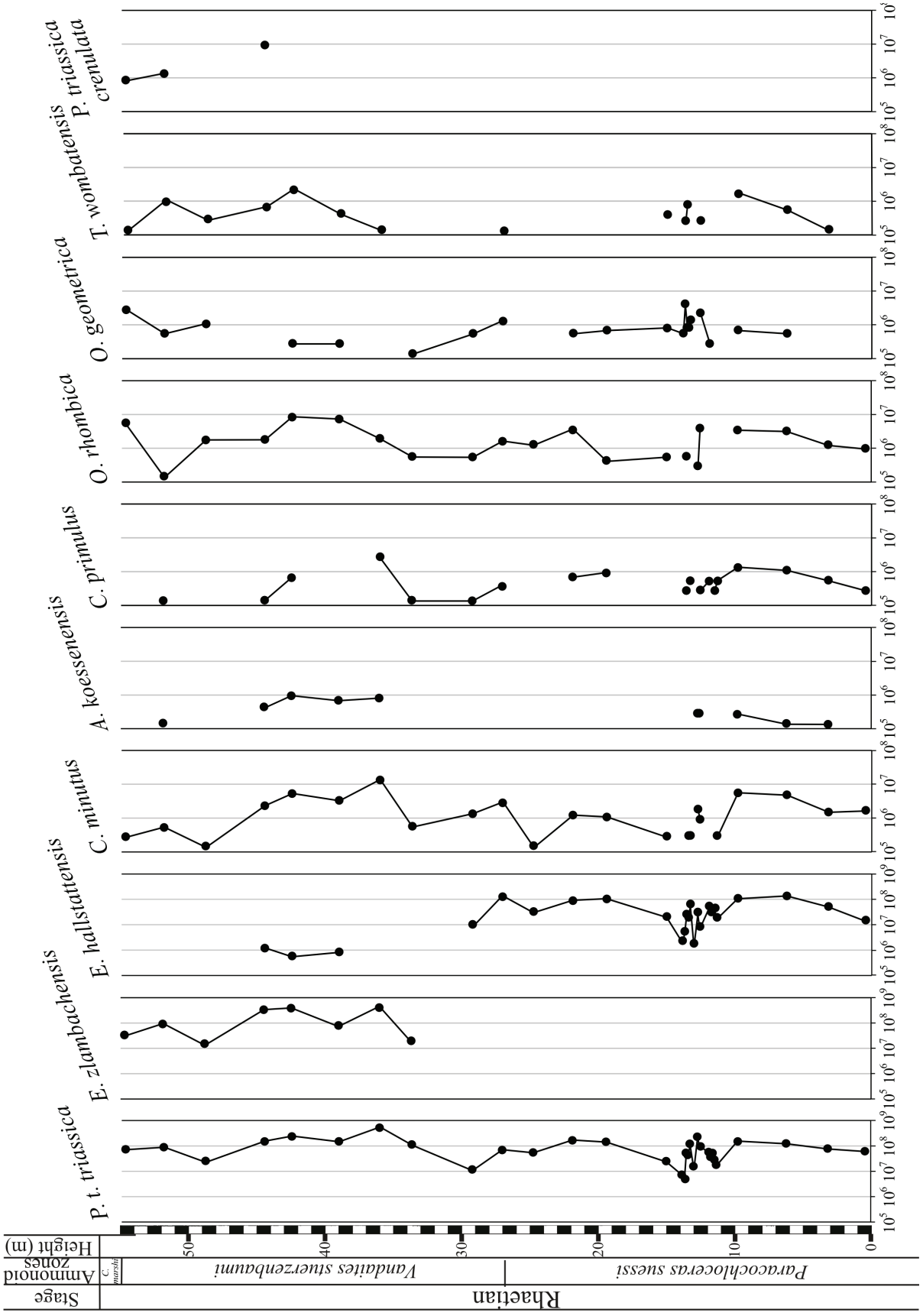

Fig. 11. Absolute abundance of the species present in the nannofossils assemblage at the Zlambach section.

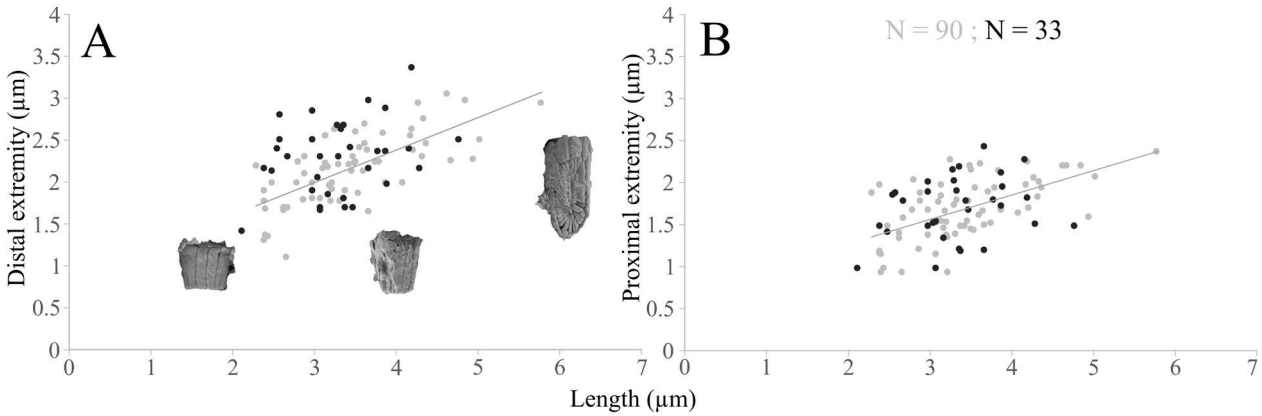

Fig. 12. Cross plot of the length of *E. hallstattensis* (grey dots) and *E. zlambachensis* (black dots), versus: A, broad extremity (distal) width and B, narrow extremity (proximal) width.

in-between (Fig. 12). The size measurements do not show any clusters of sizes, but a rather continuous size range can be observed for both species. Figure 12 highlights the similar size range of the two species.

Calcareous nannofossil preservation and diagenetic impact

The bulk samples are composed of micritic limestones with dominantly calcite mineralogy and contain some clay minerals but barely dolomite. The sole biogenic components recognized in the sample set are calcareous nannofossils. Their identification is sometimes difficult due to partly highly abundant clay minerals, which cover the nannofossils. Some dissolution patterns are visible in the samples, such as dissolution pits, rough calcite surfaces and rounded particle edges of the abiogenic material. However, no recrystallization patterns (calcite step-growth, transitions of micrite to calcite spar, dolomitization) are visible. Therefore, a large diagenetic impact on calcareous nannofossils preservation degree and abundance can be reasonably ruled out. Moreover, the *P. t. triassica* specimens appear with all inner or outer calcite lamellae visible, which can be assigned to stage 3 (relatively good preservation degree) applying the classification of Bralower *et al.* (1991). The two *Eoconusphaera* species do not seem to be impacted by diagenesis either. Indeed, their inner structure, i.e., the lamellae, the core and the inclination of *E. zlambachensis*, is still intact and visible. The calcispheres and the coccolithophorids also appear in good preservation with their structure and all characteristic elements visible.

The impact of diagenesis was also studied through analysis of the elemental composition (Table 1) of the limestone beds. The chemical composition is similar for almost all of the samples analysed, except for sample Zl 19.9249. The latter represents a calciturbidite layer, which has a markedly higher Mg (3 wt%), Fe (1.3 wt%), Si (2.8 wt%), Al (1.2 wt%) and K (0.3 wt%) content and lower Ca content (15.9 wt%), compared to the other samples. These have a high Ca content ranging between 30.6 and 39 wt%, as well as minor Mg (0.7–1.8 wt%), Fe (0.2–0.6 wt%), Si (0.5–1.6 wt%), Al (0.2–0.7 wt%) and K (0.1–0.2 wt%) contents. This composition reflects the dominant $CaCO_3$ mineralogy with a minor presence of dolomite, Fe-(hydr) oxides and clay minerals (see also Kovács et al. 2020). The Al/Ca vs. Fe/Ca cross-plot shows a positive linear correlation ($R^2 = 0.82$; Fig. 13A), indicating that all Fe has a continental-detrital origin and thus cannot be used as an indicator for diagenesis. However, the relatively high Na (268–605 ppm) and Sr (630–1156 ppm) contents and the low Mn (221–475 ppm) content (Fig. 13B) argue against overprinting of the pristine chemical composition of the rocks during burial diagenesis, which would lead to a depletion in Na and Sr and enrichment in Mn (e.g. Baldermann *et al.* 2015; Kovács *et al.* 2020; Demangel *et al.* 2020).

Discussion

Upper Triassic Calcareous nannofossil affinity

The qualitative investigation of the calcareous nannofossils at the Zlambach section brings new information to understand the affinities of the Upper Triassic calcifiers. Orthopithonelloideae and Obliquipithonelloideae were suggested to belong to the calcifying dinoflagellates (Janofske 1992) as *O. misurinae* presents a circular opening similar to an archeopyle (opening in the wall typical for the dinocyst) and *O. prasina* presents a wall ultrastructure close to the wall of Cretaceous

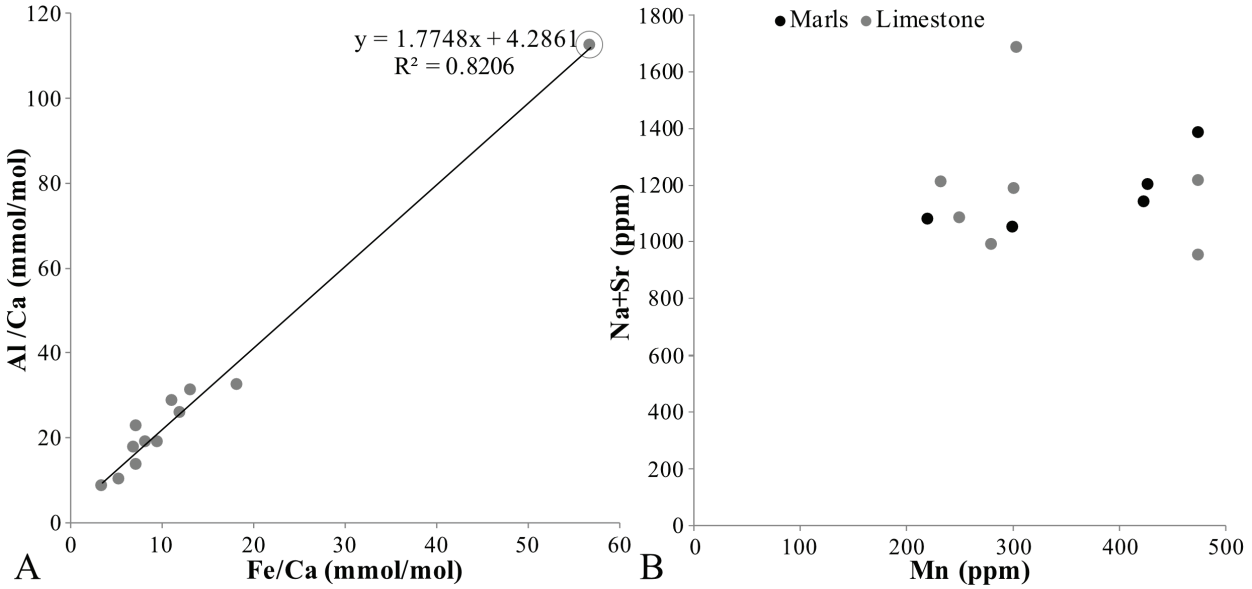

Fig. 13. Cross plots of A: Al/Ca (mmol/mol) and Fe/Ca (mmol/mol), R^2 is given without the outstanding point circled; and B: Na+Sr (ppm) versus Mn (ppm).

dinocysts (Janofske 1992). Thus, the Late Triassic species, *Orthopithonella geometrica* and *Obliquipithonella rhombica,* were first described as calcareous cysts of dinoflagellates. Later, this affinity was questioned as characteristics from the dinocysts, such as the opening in the wall (archeopyle) or the tabulation (number and position of articulated plates), are not always recognized. Calcareous dinoflagellate cysts are resistant to adverse conditions (Fensome *et al.* 1993) and their formation is often triggered by changes in temperature, nutrients and/or light availability (Pfiester & Anderson 1987). Over *V. stuerzenbaumi* Zone (middle Rhaetian), distinct fauna changes and the occurrence of a high latitude palynological assemblage suggest deposition during cool environmental conditions (Kürschner *et al.* 2008). Additionally, the carbonate bio-productivity of the platform dropped due to the reduced availability of nutrients (see below sub-chapter *Prinsiopshaera triassica triassica size decrease*). Those palaeoenvironmental perturbations occurred along with the increase in the abundance of *Orthopithonella geometrica* and *Obliquipithonella rhombica* and the decrease of the other calcareous nannofossils supporting an affinity of those two species to the Dinophyceae.

Thoracosphaera wombatensis was first described and included within the Dinophyceae via its generic assignment by Bralower *et al.* (1991). Later on, Streng *et al.* (2004) suggested that this form could represent a species of *Schizosphaerella* due to its hat shape similar to the valve of S. punctulata. However, the wall-structure of *T. wombatensis* is very different from that of *S. punctulata* and it is now included within Thoracosphaeraceae (Gottschling *et al.* 2008). In the studied section, *T. wombatensis* is rare but its abundance shows similar fluctuations compared to the other calcareous dinoflagellates, especially *O. rhombica*. However, the abundance of *T. wombatensis* at the topmost section does not increase as the abundance of *Orthopithonella geometrica* and *Obliquipithonella rhombica* does. Indeed, the calcareous sphere produced by the *Thoracosphaera* species corresponds to a coccoid, vegetative phase with a calcareous wall produced after asexual division (Tangen *et al.* 1982) and not triggered by environmental changes. This different mode of formation might explains the inverse abundance variation at the top of the section subjected to a presumed cooling event and decrease in nutrient availability. The calcareous wall formation of the extant species *Thoracosphaera heimii* is described with rhombic and irregular polygons, representing early grown crystals. Such structure can be observed in *T. wombatensis* in the NCA (Fig. 7) (Demangel *et al.* 2020). Those observations are in favour of an assignment of *T. wombatensis* to the Dinophyceae.

The *Eoconusphaera* species observed in this study are classified as nannolith due to their unknown origin. However, this Upper Triassic conical genus can be compared to the three other conical genera present in the Mesozoic rock record, i.e., *Mitrolithus*, *Calcivascularis* (Lower Jurassic) and *Conusphaera* (uppermost Jurassic to Lower Cretaceous). They are all classified as coccoliths and, like *Eoconusphaera* sp., they present an outer cycle of vertical, non-imbricated elements described as a protolithic rim. The rim of all those conical forms

presents a broad range of sizes including a low rim of ~ 2 μm size, similar to the protolith rim of the Upper Triassic coccolith ancestor *Crucirhabdus minutus*. Additionally, the abundances of *Eoconusphaera* sp. and *C. minutus* at the Zlambach section show a high co-variation (see at 27 m, 42 m and 44 m). However, some doubt remains regarding the affinity of the *Eoconusphaera* species due to the opposite proliferation, i.e. low abundance for the coccolithphorirds and high one for *E. zlambachensis* even competing with the dominant *P. t. triassica.*

Calcareous nannofossil evolution during the Rhaetian at the Zlambach section

Studies on Upper Triassic calcareous nannofossils are mainly concentrated on the Norian/Rhaetian boundary and the Rhaetian stage. As highlighted in Figure 14, only a few studies focus on Carnian and none on lower Norian (Lacian) records. Additional investigations on Carnian and Norian sediments are needed to better constrain the evolution of early calcifiers. The early calcareous nannofossils seem to evolve slowly in diversity with a total of ten species common in the Upper Triassic assemblages occurring an interval over ~ 36 Ma, from Carnian to the Triassic/Jurassic boundary.

The cysts from calcareous dinoflagellates present a low diversification with two species in the lower Carnian (Cordevolian), i.e., *Obliquipithonella prasina* (Janofske 1992) and, *Orthopithonella misurinae* (Janofske 1992), occurring in the Western Tethys and seem to disappear during the Mid-Carnian extinction event (Fig. 14). The sister taxa *Orthopithonella geometrica* (Jafar 1983) is observed from the middle Norian (Alaunian 3) in the Western Tethys (Demangel *et al*. 2020) and the Southern Tethys Ocean (Bralower et al. 1991). *Obliquipithonella rhombica* (Janofske 1987) evolved in the lower Rhaetian and was observed only in the Western Tethys (Demangel *et al*. 2020). In the Zlambach section, both *O. geometrica* and *O. rhombica* show a low abundance with *O. rhombica* being more frequent. The Thoracosphaeroideae are represented only by *T. wombatensis* in very low abundance. This species was first described from the Southern Tethys in Rhaetian sediments (Bralower *et al*. 1991) but it also occurs in the Western Tethys from the middle Norian (Fig. 14) (Demangel *et al*. 2020).

The incertae sedis, *Prinsiosphaera triassica triassica*, is first described from the middle Norian in the Western Tethys (Fischer *et al*. 1967) and observed from the Rhaetian in the Southern Tethys (Bralower *et al*. 1991). In all localities analysed, this species dominates the assemblages of calcareous nannofossils (Bralower *et al*. 1991; Gardin *et al*. 2012; Preto *et al*. 2013; Demangel *et al*. 2020). In the Western Tethys, the percentages of *P. t. triassica* composing the rocks (wt% $CaCO_{3P.\ t.\ triassica}$) were estimated in Italian (Pizzo Mondello, Pignola-Abriola) and Austrian sections (Steinbergkogel, Zlambach). In the Austrian section, during the Norian, *P. t. triassica* accounts for less than 2% of the rocks reaching 5% until the early Rhaetian (*P. suessi* Zone) (Demangel et al., 2020). At the Zlambach section, the wt% $CaCO_{3P.\ t.\ triassica}$ varies around 5% with two increases to around 15% in the lower Rhaetian (*P. suessi* Zone) and up to 18% in the middle Rhaetian (*V. stuerzenbaumi* Zone). Those values corroborate the quantification of Preto *et al*. (2013) at Pignola-Abriola (Lagonegro Basin, Italy), where wt% $CaCO_{3P.\ t.\ triassica}$ fluctuates between 0 and 20% in the Norian and Rhaetian. *Prinsiosphaera triassica triassica* did not reach rock-forming abundance in the Hallstatt and Lagonegro basins at this time.

The subspecies *Prinsiosphaera triassica crenulata* was first described by Jafar (1983) from the Zlambach section. Named after its crenulated or wavy structure (Fig. 4), the subspecies has a spherical shape made of wavy striations, corresponding to calcite lamellae oriented parallel to each other. Bralower *et al*. (1991) rejected this subspecies and hypothesized that these structures are the result of etching and overgrowth processes associated with diagenesis. However, our observations show striation features similar to those reported by Jafar (1983), under both LM and SEM, which supports the validity of the subspecies *P. triassica crenulata*. From our observation, this species occurs in the middle Rhaetian (*V. stuerzenbaumi* Zone) in a low abundance. *P. triassica crenulata* was also reported from the southern Tethys Ocean (the North West Shelf of Australia) with a distinct acme in the Rhaetian (Rutledge *et al*. 2015). Ten specimens were measured and all have a diameter between 12 and 13 μm, which is higher than the mean diameter of 7 μm reported by Jafar (1983). More size measurements from different localities and time intervals are needed to confirm the potential specific size of *P. triassica crenulata*.

From the lower Rhaetian (*P. suessi* Zone), *Eoconusphaera hallstattensis* (Demangel et al. 2020), and from the middle Rhaetian (*V. stuerzenbaumi* Zone), *Eoconusphaera zlambachensis,* are present in the western and southern Tethys Ocean. We recently revised their taxonomy (Demangel *et al*. 2021). In the Zlambach section, *E. zlambachensis* is more abundant than *E. hallstattensis*, reaching maximum abundances in the middle Rhaetian (*V. stuerzenbaumi* Zone). Additionally, the first occurrence of *P. triassica crenulata* in the middle *V. stuerzenbaumi* Zone (middle Rhaetian) corresponds to the last occurrence of *E. hallstattensis*. Throughout the Rhaetian, three zones can

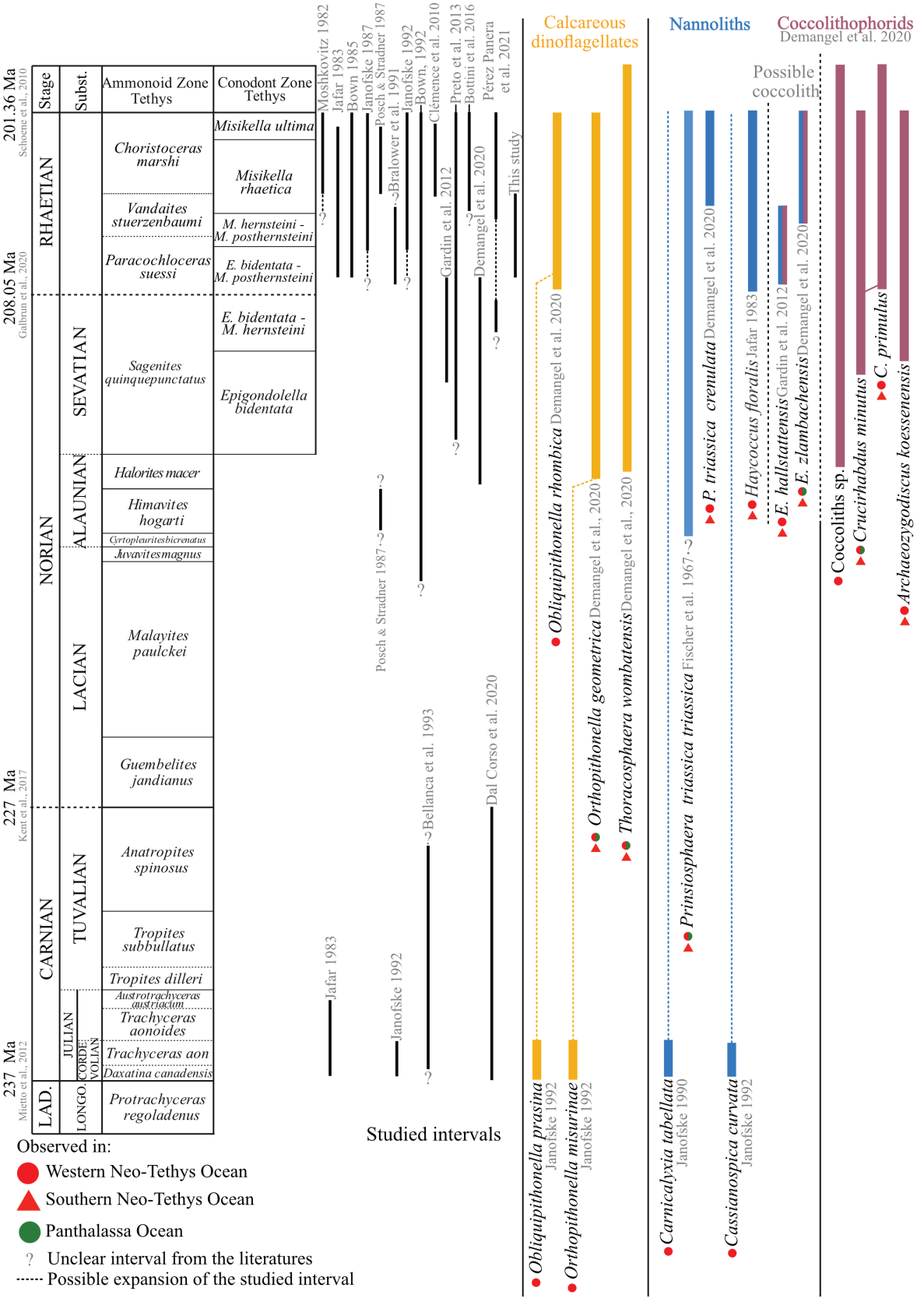

Fig. 14. Late Triassic biozonation based on ammonoids and conodonts for the Tethyan realm (Galbrun *et al.* 2020; Ogg *et al.* 2020) along with the calcareous nannofossils ranges of the Upper Triassic.

be recognized as follows: first *E. hallstattensis* alone, then *E. hallstattensis*/*E. zlambachensis* and last *E. zlambachensis*/*Prinsiosphaera triassica crenulata*. Those three taxa could be used as biostratigraphical markers in the Rhaetian in the Northern Calcareous Alps.

Known since the middle Norian, the coccolithophorids evolved slowly in diversity throughout the Upper Triassic (Demangel *et al*. 2020) (Fig. 14). During the Norian, two species occurred with low abundance: *Crucirhabdus minutus* (Jafar 1983) and then *Archaeozygodiscus koessenensis* (Bown 1985). From the lower Rhaetian, a third species, *Crucirhabdus primulus* (Prins 1969), appeared and it is the only coccolithophores species known to have survived the end-Triassic mass extinction (Fig. 14). If the two *Eoconusphaera* species are considered as coccolithophorids (see above), the diversity of the early coccolithophorids would be higher and faster than previously expected, reaching a diversity of five species in ~7.2 Myr. During the middle Rhaetian, coccolithophorids show a slight increase in abundance reaching 7.5% of relative abundance, but they remain the least abundant type of calcareous nannofossils during the Late Triassic. *Crucirhabdus minutus*, the suggested ancestor, is the far most abundant coccolith species.

Calcareous nannofossil abundance through the Rhaetian

During the Rhaetian, within an assemblage of more than ten species, only two are present in high abundance, i.e., *P. t. triassica* and *E. zlambachensis*. Quantifications of Upper Triassic calcareous nannofossils are rare to non-existent for some areas, making a comparison between different sections almost impossible. The nannofossil accumulation rate fluctuates around 9×10^9 (nannos / m^2 / yr) and reaches a maximum at 3.5×10^{10} (nannos / m^2 / yr). Those values seem considerable as they correspond to the lower Jurassic nannofossil accumulation rate fluctuating around 10^9 (nannofossil m^2 yr^{-1}) during the Sinemurian (Suchéras-Marx *et al*. 2019b).

The carbonate flux linked to the abundance of *P. t. triassica* seems significant, but comparisons are not possible as no previous carbonate flux linked to the calcareous nannofossil abundance exists for the Triassic period. The carbonate flux linked to the calcareous nannofossil abundance during their early evolution, i.e. Upper Triassic to Lower Jurassic are very informative, however, they are inaccurate due to different uncertainties. On the one hand, information on deep-time oceanic palaeoenvironmental conditions is difficult to assess. Dissolution of calcium carbonate occurs in the water column with increasing ease below the calcite saturation depth and even more below the carbonate compensation depth. Additionally, depending on the depositional depth, further dissolution may occur on the seafloor and in the subsurface sediments during early burial. The intensity of dissolution affecting the studied sediments before their burial is difficult to evaluate, however, the dissolution is of minor significance for sediments deposited in shallow palaeoenvironments. After deposition of the calcium carbonate shells, the diagenetic alteration during burial further impacts the preservation of the calcareous nannofossils.

The stage of diagenesis could be constrained with geochemical proxies but uncertainty remains on its impact on the calcareous nannofossils abundance and the corresponding shape and size measurements of the specimens, which could partially dissolve on the edges and thus present a smaller size than originally. The diagenetic alteration also leads to fragmentary specimens that are difficult to include in the counting. Finally, the sedimentation rate for the Upper Triassic is difficult to assess precisely and is thus often considered as a fixed value throughout the studied section. On the other hand, inaccuracy in the carbonate flux may also happen due to possible human errors during the sample preparation and counting.

Size variation of the nannoliths

The Eoconusphaeraceae. Bralower (1991) and Kristan-Tollmann (1995) have reported on the evolution of respectively *E. hallstattensis* and *E. zlambachensis* from a short, stubby shape (length: 2 to 4 µm, average: 3 µm) to a narrow, elongated form (length: 3 to 6 µm, average: 5 µm). Our results reveal a broad range of sizes for both *Eoconusphaera* species, ranging from short and stubby to long and narrow shapes with a broad range of medium sizes in-between. Our measurements corroborate the average size range of 3 to 5 µm previously reported by Bralower *et al*. (1991), however, in our study, no temporal evolution of the Eoconusphaeraceae shapes were observed, as many sizes were found in single samples (Fig. 12).

Prinsiosphaera triassica triassica *size decrease*

After its appearance in the middle Norian, *P. t. triassica* has a constant size (Demangel *et al*. 2020) but from the top of the *P. suessi* Zone a decrease in size is recorded, from 9 to 6 µm on average, which is accompanied by the disappearance of the very large size group of *P. t. triassica* (10–13µm). During the latest Rhaetian (*C. marshi* Zone), Clémence et al. (2010) also reported: 1, a decrease in the size of *P. t. triassica* until the extinction of the species; and 2, did not record very large sized

specimens in another Austrian locality (Eiberg section). During the latest Rhaetian, Bottini et al. (2016) also reported a size decrease of *P. t. triassica* in the Italian Southern Calcareous Alps (Italcementi active quarry), however, they recognized the presence of very large sized *P. t. triassica* (10–13 µm) too. They measured a decrease in size from very large (10–13 µm) to small (< 5 µm) with the smallest sizes recorded just before the Triassic/Jurassic boundary during the 'initial negative Carbon Isotope Excursion (CIE)'. The observation of very large specimens in Italy during the latest Rhaetian suggests a local perturbation in the NCA during the middle Rhaetian, which led to the size decrease of the population of *P. t. triassica*.

In our study, the size variations do not correlate with the abundance variations of the other main calcareous nannofossils (Fig. 15A). Thus, a possible competition between species seems unlikely to explain the size decrease. The size and the abundance of *P. t. triassica* do not covary, as shown for the end-Triassic mass extinction as well (Bottini *et al.* 2016), and hence most likely reflect a perturbation of nannoplankton biocalcification. Clémence et al. (2010) explained the size decrease of *P. t. triassica* observed during the late Rhaetian either by a local cooling event or a change in seawater chemistry, i.e., a lower pH value, and suggested warm seawater to be favourable for the bioproductivity of *P. t. triassica*. Calcareous nannoplanktons are highly sensitive to environmental changes (Brand 1994), such as seawater temperature and chemistry (Clémence *et al.* 2010; Peti & Thibault 2017), to nutrient and light availability (Clark & Watkins 2020; Wulff *et al.* 2020) and climatic changes (Möller et al. 2020). The effects of any of these changes are species-dependent and could lead to variations in both abundance and size.

In the Late Triassic the NCA were characterized by the long-term development of the large Dachstein carbonate platform that expanded southward over the marginal Hallstatt basin (Figs 1, 16). According

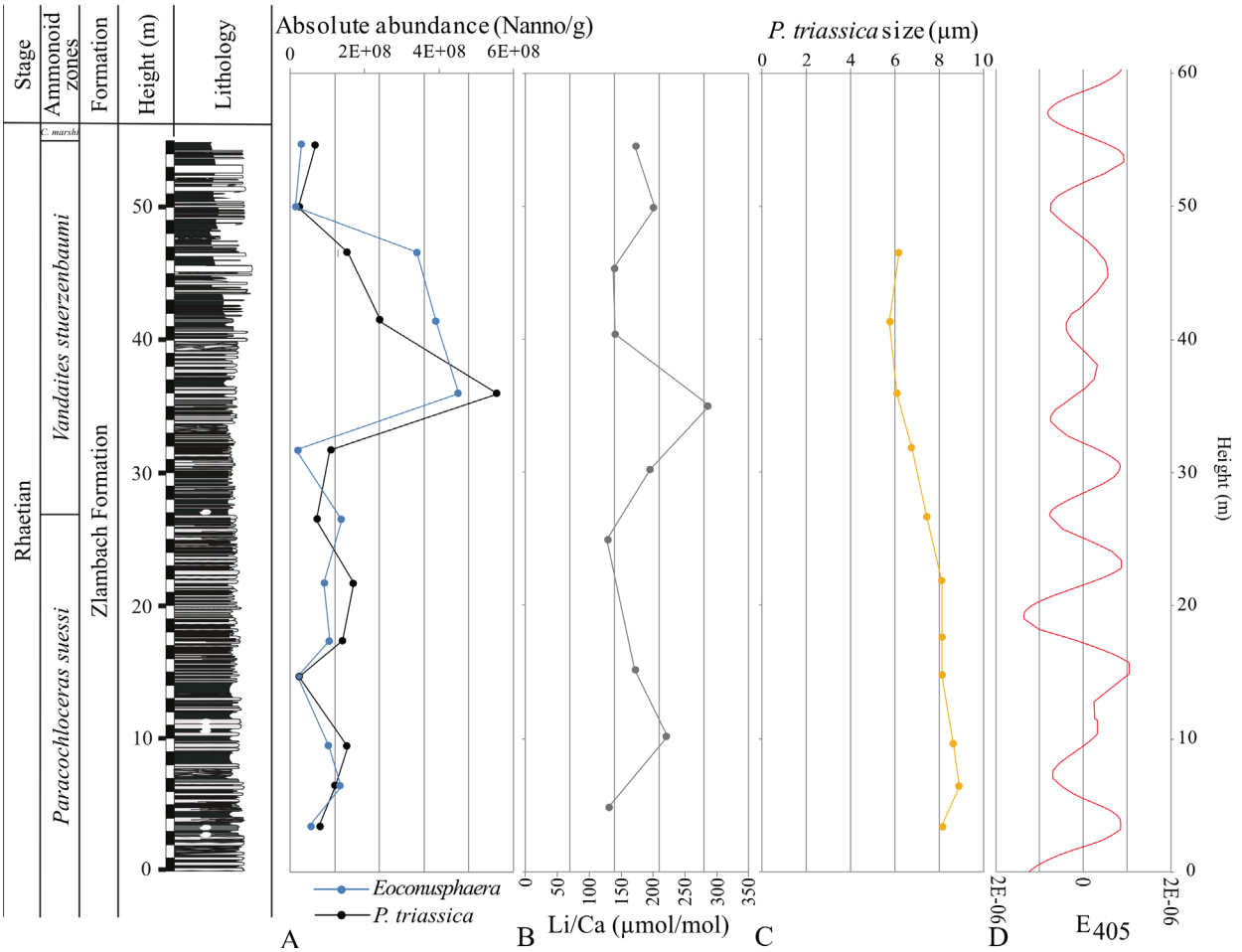

Fig. 15. Graphs showing changes in: A, absolute abundance of *P. t. triassica* and the two Eoconusphaera species (*E. hallstattensis*, *E. zlambachensis*) (Nanno/g); B, Li/Ca ratios; C, size variation of *P. t. triassica*; and D, eccentricity cycles calculated at Zlambach from magnetosusceptibility measurements by Galbrun *et al.* (2020).

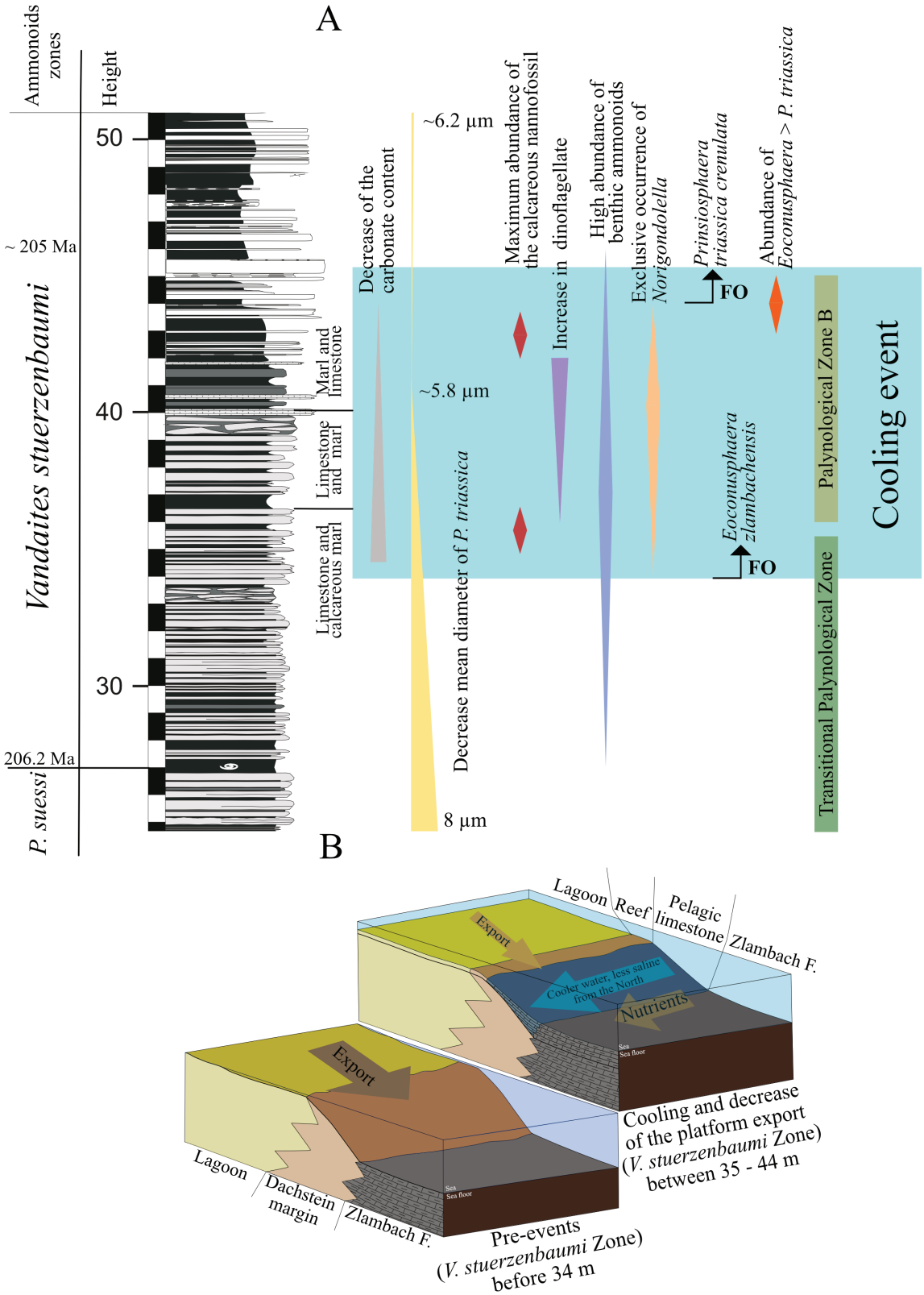

Fig. 16. Main events during the Rhaetian at the Zlambach section: A, schematic representation of the First Occurrences and qualitative abundance fluctuation of the microfossils, conodont and carbonate content suggesting a cooling phase during the Rhaetian at the Zlambach section; B, schematic 3D block diagrams representing the evolution of the Dachstein carbonate platform and the suggested events during the Rhaetian at Zlambach, i.e., decrease of the carbonate export from the platform and cooling event.

to Krystyn *et al.* (2009), during the middle Rhaetian the progradation stopped and a pelagic limestone cover developed over the former platform margin. While, Mette *et al.* (2019) suggest a continuation of the carbonate production on the platform until the late Rhaetian (C. marshi zone). A platform productivity drop should have led to a reduction in the export of peri-platform carbonate mud to the adjacent Zlambach basin. In the studied section, this process is reflected by: 1, pulses of increasing terrigenous input at around 36 m; and 2, a change from calcareous marlstones to marlstone at 36 m in the profile (Fig. 16). The Li/Ca ratio (Fig. 15B), a sensitive indicator of continental influx, also highlights a short increased in terrestrial contribution, shown by higher values at 36 m (Kovács et al. 2020). Moreover, the beds cropping out between 35 m and 45 m record an unusual abundance of the ammonoids, especially *Cochloceras, Cycloceltites* and *Vandaites* (Richoz & Krystyn 2015; Galbrun et al. 2020), and the conodonts *Norigondolella* and *Epigondolella*, which are otherwise only sporadically represented or even missing throughout the remaining section. A concurrent burst of the dinoflagellate cysts *Heibergella aculeata* and *Dapcodinium priscum* as well as a turnover in the miospore record were interpreted by Kürschner *et al.* (2008) as indications of a cooling event and a related transition to more humid conditions. We suggest an inflow of cooler water from the northern areas importing those new assemblages and possibly leading to a change in salinity, which influenced the calcareous producers. Those palaeo-environment changes could have added stress on the calcifiers community, which (after a steady size reduction starting at 22 m of the section) would explain the noticeable size minimum of *P. t. triassica* between 36 and 42 m up-section.

Conclusions

The Northern Calcareous Alps bear a great potential to study the early evolution of calcareous nannofossils. The calcareous nannofossil assemblage records a maximum abundance during the middle Rhaetian with up to 3.5×10^{10} (nannos / m^2 / yr), which comes along with the first occurrence of *E. zlambachensis* (oblique inner lamellae) within *V. stuerzenbaumi* Zone, henceforth dominating over *E. hallstattensis* (vertical inner lamellae). *Prinsiosphaera triassica crenulata* was observed with distinct striation patterns, confirming the validity of this subspecies initially described by Jafar (1983). The disappearance of the very large sized *P. t. triassica* (10–13 µm) and a continuous decrease in the size of *P. t. triassica* are recorded in the lower Rhaetian (*P. suessi* Zone; the base of Zlambach section). The minimum size is reached in the middle Rhaetian and continues until the extinction of *P. t. triassica* at the Triassic/Jurassic boundary (Clémence *et al.* 2010), which may be the result of regional palaeo-environmental changes. A middle Rhaetian (*V. stuerzenbaumi* Zone) cooling event, as evidenced by a striking change in ammonoids, dinoflagellates cysts and miospores assemblages could have impacted the size of the main Upper Triassic nannolith *P. t. triassica*, affected further by the co-evolution and competition of the Eoconusphaeraceae. During the early and middle Rhaetian, *P. t. triassica* did not reach rock-forming abundance and contributed with < 20% to the rock record. We suggest good adaptability of *P. t. triassica* and other nannoliths to warm and proximal water masses having a higher nutrient availability.

Acknowledgements. – This research was supported by the Austrian Science Foundation (Project P 29497-P29; grant to Sylvain Richoz) and by the 'RESPECT' (A major evolutive Revolution: the Emergence and Spreading of PElagic Calcifiers in the late Triassic) PICS-CNRS project to Silvia Gardin. The SEM analyses were supported by the Royal Physiographic Society of Lund (grant to Isaline Demangel). We thank Nicolas Thibault for the valuable scientific discussion and are thankful for the thorough reviews of Drs Suchéras-Marx, Young, Thibault and Mette.

References

Baldermann, A., Deditius, A.P., Dietzel, M., Fichtner, V., Fischer, C., Hippler, D., Leis, A., Baldermann, C., Mavromatis, V., Stickler, C.P. & Strauss, H. 2015: The role of bacterial sulfate reduction during dolomite precipitation: Implications from Upper Jurassic platform carbonates. *Chemical Geology 412*, 1–14.

Baldermann, A., Grießbacher, A.C., Baldermann, C., Purgstaller, B., Letofsky-Papst, I., Kaufhold, S. & Dietzel, M. 2018a: Removal of Barium, Cobalt, Strontium, and Zinc from Solution by Natural and Synthetic Allophane Adsorbents. *Geosciences 8*, 1–22.

Baldermann, A., Mavromatis, V., Frick, P.M. & Dietzel, M. 2018b: Effect of aqueous Si/Mg ratio and pH on the nucleation and growth of sepiolite at 25°C. *Geochimica et Cosmochimica Acta 227*, 211–226.

Baldermann, A., Mittermayr, F., Bernasconi, S.M., Dietzel, M., Grengg, C., Hippler, D., Kluge, T., Leis, A., Lin, K., Wang, X., Zünterl, A. & Boch, R. 2020: Fracture dolomite as an archive of continental palaeo-environmental conditions. *Communications Earth and Environment 1*, 35.

Bellanca, A., Di Stefano, E., Di Stefano, P., Erba, E., Neri, R. & Pirini Radrizzani, C. 1993: Ritrovamento di 'Calcisfere' e nannofossili calcarei in terreni carnici della Sicilia. *Paleopelagos 3*, 91–96.

Bordiga, M., Bartol, M. & Henderiks, J. 2015: Absolute nannofossil abundance estimates: quantifying the pros and cons of different techniques. *Revue de micropaléontologie 58*, 155–165.

Bottini, C., Jadoul, F., Rigo, M., Zaffani, M., Artoni, C. & Erba, E. 2016: Calcareous nannofossils at the Triassic/Jurassic boundary: Stratigraphic and paleoceanographic characterization. *Rivista Italiana di Paleontologia e Stratigrafia (Research in Paleontology and Stratigraphy) 122*, 141–164.

Bown, P.R. 1985: Archaeozygodiscus gen. Nov. and other Triassic coccoliths. *INA Newsletter* 32–35.

Bown, P.R. 1987: The structural Development of Early Mesozoic Coccoliths and its Evolutionary and Taxonomic Significance. *Abhandlungen der Geologischen Bundesanstalt 39*, 33–49.

Bown, P.R. 1992: Late Triassic-Early Jurassic calcareous nannofossils of the Queen Charlotte Islands, British Columbia. *Journal of Micropaleontology 11*, 177–188.

Bown, P.R. & Cooper, M.K.E. 1998: Jurassic. In, Bown, P. R. (ed.) Calcareous Nannofossil Biostratigraphy. *British Micropalaeontological Society Publication Series* 34–85.

Bralower, T.J., Bown, P.R. & Siesser, W.G. 1991: Significance of Upper Triassic nannofossils from the Southern Hemisphere (ODP Leg 122, Wombat Plateau, N.W. Australia). *Marine Micropaleontology 17*, 119–154.

Brand, U. & Veizer, J. 1980: Chemical diagenesis of a multicomponent carbonate-system – 1: Trace elements. *Journal of Sedimentary Petrology 50*, 1219–1236.

Brand, L.E. 1994: Physiological ecology of marine coccolithophores. In Winter, A. & Siesser, W.G., (eds) *Coccolithophores*, Cambridge University Press, Cambridge 39–49.

Clark, W. B. & Watkins, D. K. 2020: A quantitative analysis of calcareous nannofossils across a late oligocene paleolatitudinal transect of the North Atlantic Ocean. *Marine Micropaleontology 158*, 101892.

Clémence, M.E., Gardin, S., Bartolini, A., Paris, G., Beaumont, V. & Guex, J. 2010: Bentho-planktonic evidence from the Austrian Alps for a decline in sea-surface carbonate production at the end of the Triassic. *Swiss Journal of Geosciences 103*, 293–315.

Clopper, C.J. & Pearson, E.S. 1934: The use of confidence or fiducial limits illustrated in the case of the binomial. *Biometrika 26*, 404–413.

Dal Corso, J., Preto, N., Agnini, C., Hohn, S., Merico, A., Willems, H., Gianolla, P., 2020: Rise of calcispheres during the Carnian Pluvial Episode (Late Triassic). *Global and Planetary Change 200*, 103453.

Deflandre, G.M. 1970: Présence de nannofossiles calcaires (coccolithes et Incertae sedis) dans le Siluro-dévonien d'Afrique du Nord. *Comptes rendus hebdomadaires des séances de l'Académie des sciences. Série D, Sciences naturelles* 2916–2921.

Demangel, I., Kovács, Z., Richoz, S., Gardin, S., Krystyn, L., Baldermann, A. & Piller, W. E. 2020: Development of early calcareous nannoplankton in the Northern Calcareous Alps (Austria) in the Late Triassic. *Global and Planetary Change 193*, 103254.

Demangel, I., Howe, R., Gardin, S. & Richoz, S. 2021: *Eoconusphaera hallstattensis*, new species, and review of the Rhaetian genus *Eoconusphaera*. *Journal of Nannoplankton Research 39*, 77–87.

Di Nocera S. & Scandone P. 1977: Triassic nannoplankton limestones of deep basin origin in the central Mediterranean region. *Palaeogeography, Palaeoclimatology, Palaeoecology 21*, 101–111.

Erba, E. 2006: The first 150 million years history of calcareous nannoplankton: Biosphere-geosphere interactions. *Palaeogeography, Palaeoclimatology, Palaeoecology 232*, 237–250.

Fischer, A.G., Honjo, S. & Garrison, R.A.E. 1967: *Electron Micrographs of Limestones and their Nannofossils*. Princeton University Press, Princeton.

Frech, F. 1890: Die Korallen der Trias. – I. Die Korallen der juvavischen Triasprovinz. *Paläontographica 37*, 1–116.

Galbrun, B., Boulila, S., Krystyn, L., Richoz, S., Gardin, S. & Bartolini, A. 2020: « Short » or « long » Rhaetian? Astronomical calibration of Austrian key sections. *Global and Planetary Change 192*, 103253.

Gardin, S., Krystyn, L., Richoz, S., Bartolini, A. & Galbrun, B. 2012: Where and when the earliest coccolithophores? *Lethaia 45*, 507–523.

Goddéris, Y., Donnadieu, Y., de Vargas, C., Pierrehumbert, R. T., Dromart, G. & van de Schootbrugge, B. 2008: Causal or casual link between the rise of nannoplankton calcification and a tectonically-driven massive decrease in Late Triassic atmospheric CO_2? *Earth and Planetary Science Letters 267*, 247–255.

Golonka, J. 2007: Late Triassic Early Jurassic palaeogeography of the world. *Palaeogeography, Palaeoclimatology, Palaeoecology 244*, 297–307.

Gottschling, M., Renner, S.S., Meier, K.J.S., Willems, H., Keupp, H., 2008: Timing deep divergence events in calcareous dinoflagellates. *Journal of Phycology 44*, 429–438. https://doi.org/10.1111/j.1529-8817.2008.00479.x

Hammer, Ø., Harper, D.A.T. & Ryan, P.D. 2001: PAST: paleontological statistics software package for education and date analysis. *Palaeontologia Electronica 4*, 1–9.

Hannisdal, B., Henderiks, J. & Liow, L.H. 2012: Long-term evolutionary and ecological responses of calcifying phytoplankton to changes in atmospheric CO_2. *Global Change Biology 18*, 3504–3516.

Iglesias-Rodriguez, M.D., Halloran, P.R., Rickaby, R.E.M., Hall, I.R. & Colmenero-Hidalg, E. 2008: Phytoplankton Calcification in a High-CO_2 World. *Science 320*, 336–340.

Jafar, S.A. 1983: Significance of Late Triassic calcareous Nannoplankton from Austria and Southern Germany. *Neues Jahrbuch für Geologie und Paläeontologie 166*, 218–259.

Janofske, D. 1987: Kalkige Nannofossillien aus der ober-Trias (Rhät)der Nördlichen kalkalpen. *Berliner geowissenschatliche Abhandlungen 86*, 45–67.

Janofske, D. 1990: Eine neue 'Calcisphaere' Carnicalyxia tabellata n.g. n.sp. aus den Cassianer Schichten (Cordevol, unteres Karn) der Dolomiten. *Berliner Geowissenschaftliche Abhandlungen 124*, 259–269.

Janofske, D. 1992: Kalkiges Nannoplankton, insbesondere kalkige Dinoflagellaten-Zysten der alpinen Ober-Trias: Taxonomie, Biostratigraphie und Bedeutung für die Phylogenie der Peridiniales. *Berliner Geowissenschaftliche Abhandlungen 4*, 1–53.

Kovács, Z., Demangel, I., Richoz, S., Hippler, D., Baldermann, A. & Krystyn, L. 2020: New constraints on the evolution of $^{87}Sr/^{86}Sr$ of seawater during the Upper Triassic. *Global and Planetary Change 192*, 103255.

Kristan-Tollmann, E. 1964: Die Foraminiferen aus rhätischen Zlambachmergeln der Fischerwiese bei Aussee, Salzkammergut. *Jahrbuch der Geologischen Bundesanstalt 10*, 1–189.

Krystyn, L. 1987: Zur Rhät-Stratigraphie in den Zlambach-Schichten (vorläufiger Bericht). *Österreichische Akademie der Wissenschaften, Sitzungsberichte der Mathematisch-Naturwissenschaftlichen Klasse*, *Abteilung 1*, 196, 21–36.

Krystyn, L. 1991: Die Fossillagerstätten der alpinen Trias. *In*: Nagel, D., Rabeder, G., (Eds): Exkursionen im Jungpaläozoikum und Mesozoikum Österreichs, *Österreichische Paläontologische Gesellschaft*, 23–78.

Krystyn, L. & Kuerschner, W. M. 2005: Biotic events around the Norian – Rhaetian boundary from a Tethyan perspective. *Albertiana 32*, 17–20.

Krystyn, L., Mandl, G.W. & Schauer, M. 2009: Growth and termination of the Upper Triassic platform margin of the Dachstein area (Northern Calcareous Alps, Austria). *Austrian Journal of Earth Sciences 103*, 23–33.

Kürschner, W.M., Krystyn, L. & Richoz, S. 2008: An integrated palaeontological, geochemical and palynological study of the Rhaetian Zlambach marls in the Northern Calcareous Alps (Austria). *Berichte geologischen Bundesanstalt 76*, 13–14.

Mandl, G. W. 2000: The alpine sector of the Tethyan shelf – examples of Triassic to Jurassic sedimentation and deformation from the Northern Calcareous Alps. *Mitteilungen der Österrike Geologie Gesellschaft 92*, 61–77.

Matzner, C. 1986: Die Zlambach-Schichten (Rhät) in den Nördlichen Kalkalpen: Eine Plattform-Hang-Beckenentwicklung mit allochthoner Karbonatsedimentation. *Facies 14,* 1–104.

Mette, W., Clémence, M-E., Thibault, N., Korte, C., Konrad, B. & Ullmann, C. V. 2019: Sedimentology, carbon isotope stratigraphy and micropalaeontology of the Rhaetian Zlambach Formation – Implications for the Dachstein carbonate platform development (Northern Calcareous Alps, Austria). *Sedimentary Geology 382*, 47–60.

Moshkovitz, S. 1982: On the findings of a new calcareous nannofossil (Conusphaera zlambachensis) and other calcareous organisms in the Upper Triassic sediments of Austria. *Eclogae Geologicae Helvetiae 75*, 611–619.

Möller, C., Bornemann, A., Mutterlose, J. 2020: Climate and paleoceanography controlled size variations of calcareou nannofossils during the Valanginian Weissert Event (Early Cretaceous). *Marine Micropaleontology 157*, 101875.

Nakada, R., Ogawa, K., Suzuki, N., Takahashi, S. & Takahashi, Y. 2014: Late Triassic compositional changes of eolian dusts in the pelagic Panthalassa: response to the continental climatic change. *Palaeogeography, Palaeoclimatology, Palaeoecology 393*, 61–75.

Ogg, J.G. 2012: Triassic. In: Gradstein, F. M., Ogg, J.G., Schmitz, M.D. & Ogg, G.M. (Eds), *The Geologic Time Scale 2012*, Elsevier, Amsterdam, 681–730.

Ogg, J.G., Chen, Z.-Q., Orchard, M. J. & Jiang, H.S. 2020: The Triassic Period. In: Gradstein, F. M., Ogg, J.G., Schmitz, M.D., Ogg, G.M. (Eds), *The Geologic Time Scale 2020*, Elsevier, Amsterdam, 903–953.

Pérez Panera, J.P., Angelozzi, G.N., Riccardi, A.C., Damborenea, S.E. & Manceñido, M.O. 2021a: Triassic calcareous nannofossils from the Arroyo Malo Formation, Neuquén Basin, Argentina. First record in South America and implications on the early evolution of the group. *12° Congreso de la Asociación Paleontológica Argentina*, Buenos Aires. Abstracts, 77.

Pérez Panera, J.P., Calvo Marcilese, L., Cuello, M.J. & Giampaoli, P. 2021b : First record of calcareous nannofossils from Chambará Formation, Pucará Group, Perú: a new biostratigraphic tool for regional correlation in the Late Triassic? *12° Congreso de la Asociación Paleontológica Argentina*, Buenos Aires. Abstracts, 92.

Peti, L. & Thibault, N. 2017: Abundance and size changes in the calcareous nannofossil Schizosphaerella – Relation to sea-level, the carbonate factory and palaeoenvironmental change from the Sinemurian to earliet Toarcian of the Paris Basin. *Palaeogeography, Palaeoclmatology, Palaeoecology 485*, 271–282.

Piller, W. 1978: Involutinacea (Foraminifera) der Trias und des Lias. *Beiträge Paläontologie Österreich 5*, 1–164.

Posch, F. & Stradner, H. 1987: Report on Triassic Nannoliths from Austria. *Abhandlungen Der Geologischen Bundesanstalt 39*, 231–237.

Preto, N., Rigo, M., Agnini, C., Bertinelli, A., Guaiumi, C., Borello, S. & Westphal, H. 2012: Triassic and Jurassic calcareous nannofossils oft he Pizzo Mondello section: A SEM study. *Rivista Italiana di Paleontologia e Stratigrafia 118*, 131–141.

Preto, N., Agnini, C., Rigo, M., Sprovieri, M. & Westphal, H. 2013: The calcareous nannofossil Prinsiosphaera achieved rock-forming abundances in the latest Triassic of western Tethys: consequences for the $\delta^{13}C$ of bulk carbonate. *Biogeosciences 10*, 6053–6068.

Prins, B. 1969: Evolution and stratigraphy of coccolothinids from the lower and middle lias. International Conference Planktonic Microfossils, *Geneva 2*, 547–558.

Richoz, R., Krystyn, L., Von Hillebrandt, A. & Martindale, R. 2012: End-Triassic crisis events recorded in platform and basin of the Austrian Alps. The Triassic/Jurassic and Norian/Rhaetian GSSPs – *Journal of Alpine Geology 55*, 321–374.

Richoz, S. & Krystyn, L. 2015: The Upper Triassic events recorded in platform and basin of the Austrian Alps. The Triassic/Jurassic GSSP and Norian/Rhaetian GSSP candidate – *Berichte der Geologischen Bundesanstalt 111*, xx-xx.

Rivero-Calle, S., Gnanadesikan, A., Del Castillo, C.E., Balch, W.M. & Guikema, S.D. 2015: Multidecadal increase in North Atlantic coccolithophores and the potential role of rising CO_2. *Science 350*, 1533–1537.

Rutledge, D. C., Cole, S., Lawrence, T. & Gard, G., 2015:A new species of Late Triassic nannofossils, Botulus triassicus, and observations on Triassic assemblages from the NW Shelf of Australia. *INA15 35*, 71.

Schettino, A. & Turco, E. 2011: Tectonic history of the western Tethys since the late Triassic. Geological Society of America *Bulletin 123*, 89–105.

Schoene, B., Guex, J., Bartolini, A., Schaltegger, U. & Blackburn, T.J. 2010: Correlating the end-Triassic mass extinction and flood basalt volcanism at the 100 ka level. Geology 35, 387–390.

Schorn, A. & Neubauer, F. 2014: The structure of the Hallstatt evaporite body (Northern Calcareous Alps, Austria): A compressive diapir superposed by strike-slip shear? *Journal of Structural Geology 60*, 70–84.

Scotese, C.R. 2004: A continental drift flipbook. *The Journal of Geology 112*, 729–741.

Streng, M., Hildebrand-Habel, T., Willems, H., 2004: A proposed classification of archeopyle types in calcareous dinoflagellate cysts. *Journal of Paleontology 78*, 456–483.

Suchéras-Marx, B., Giraud, F., Mattioli, E., Gally, Y., Barbarin, N. & Beaufort, L. 2014: Middle Jurassic coccolith fluxes: A novel approach by automated quantification. *Marine Micropaleontology 111*, 15–25.

Suchéras-Marx, B., Escarguel, G., Ferreira, J. & Hammer, Ø. 2019a: Statistical confidence intervals for relative abundances and abundance-based ratios: Simple practical solutions for an old overlooked question. *Marine Micropaleontology 151*, 101751.

Suchéras-Marx, B., Mattioli, E., Allemand, P., Giraud, F., Pittet, B., Plancq, J. & Escarguel, G. 2019b: The colonization of the oceans by calcifying pelagic algae. *Biogeosciences 16*, 2501–2510.

Tangen, K., Brand, L.E., Blackwelder, P.L., Guillard, R.R.L., 1982: *Thoracosphaera heimii* (Lohman) Kamptner is a dinophyte: observations on its morphology and life cycle. *Marine Micropaleontology 7*, 193–212.

Tollmann, K. 1995: Weitere beobachtungen an Rhätischen nannofossilien der Tethys. *Geolologisch Paläontologische Mitteilungen Innsbruck 20*, 1–10.

Wulff, L., Mutterlose, J. & Bornemann, A. 2020: Size variations and abundance patterns of calcareous nannofossils in mid Barremian black Shales of the Boreal Realm (lower Saxony Basin). *Marine Micropaleontology 156*, 101853.

Zeebe, R.E. & Caldeira, K. 2008: Close mass balance of long-term carbon fluxes from ice-core CO_2 and ocean chemitry records. *Nature Geoscience 1*, 12–315.

Zhang, S., Wang, X., Hammarlund, E. U., Wang, H., Mafalda Costa, M., Bjerrum, C.J., Connelly, J.N., Zhang, B., Bian, L. & Canfield, D.E. 2015: Orbital forcing of climate 1.4 billion years ago. *Proceedings of the National Academy of Sciences of the United States of America 112*, 1406–1413.